Bioorganic & Medicinal Chemistry 20 (2012) 1468–1474

Contents lists available at SciVerse ScienceDirect

Bioorganic & Medicinal Chemistry

journal homepage: www.elsevier.com/locate/bmc

Conjugation of cell-penetrating peptides leads to identification of anti-HIV peptides from matrix proteins

Tetsuo Narumi [a], Mao Komoriya [a], Chie Hashimoto [a], Honggui Wu [b,c], Wataru Nomura [a], Shintaro Suzuki [a], Tomohiro Tanaka [a], Joe Chiba [c], Naoki Yamamoto [d], Tsutomu Murakami [b,*], Hirokazu Tamamura [a,*]

[a] Institute of Biomaterials and Bioengineering, Tokyo Medical and Dental University, Chiyoda-ku, Tokyo 101-0062, Japan
[b] AIDS Research Center, National Institute of Infectious Diseases, Shinjuku-ku, Tokyo 162-8640, Japan
[c] Department of Biological Science Technology, Tokyo University of Science, Noda, Chiba 278-8510, Japan
[d] Yong Loo Lin School of Medicine, National University of Singapore, Singapore 117597, Singapore

ARTICLE INFO

Article history:
Received 6 December 2011
Revised 24 December 2011
Accepted 24 December 2011
Available online 2 January 2012

Keywords:
Matrix protein
Octa-arginyl group
Overlapping peptide
Anti-HIV

ABSTRACT

Compounds which inhibit the HIV-1 replication cycle have been found amongst fragment peptides derived from an HIV-1 matrix (MA) protein. Overlapping peptide libraries covering the whole sequence of MA were designed and constructed with the addition of an octa-arginyl group to increase their cell membrane permeability. Imaging experiments with fluorescent-labeled peptides demonstrated these peptides with an octa-arginyl group can penetrate cell membranes. The fusion of an octa-arginyl group was proven to be an efficient way to find active peptides in cells such as HIV-inhibitory peptides.

1. Introduction

Several anti-retroviral drugs beyond reverse transcriptase inhibitors, including effective protease inhibitors[1] and integrase inhibitors[2,3] are currently available to treat human immunodeficiency virus type 1 (HIV-1) infected individuals. We have also developed several anti-HIV agents such as coreceptor CXCR4 antagonists,[4–7] CD4 mimics,[8–10] fusion inhibitors[11] and integrase inhibitors.[12,13] However, the emergence of viral strains with multi-drug resistance (MDR), which accompanies the development of any antiviral drug, has encouraged a search for new types of anti-HIV-1 drugs with different inhibitory mechanisms.

Matrix (MA) proteins are essential for assembly of the virion shell. MA is a component of the Gag precursor protein, Pr55Gag, and is located within the viral membrane.[14,15] It has been reported that MA-derived peptides such as MA(47–59) inhibit infection by HIV,[16] and that MA-derived peptides such as MA(31–45) and MA(41–55) show anti-HIV activity.[17] In addition, Morikawa et al. report that MA(61–75) and MA(71–85) inhibit MA dimerization, a necessary step in the formation of the virion shell.[18] However, the question of whether the above MA peptides can penetrate cell membranes was not addressed in these reports. We speculate that to achieve antiviral activity it is essential that the MA-derived peptides penetrate the cell membrane and function intracellularly. In this paper, we report our design and construction of an overlapping library of fragment peptides derived from the MA protein with a cell membrane permeable signal. Our aim is the discovery of potent lead compounds, which demonstrate HIV inhibitory activity inside the host cells.

2. Materials and methods

2.1. Peptide synthesis

MA-derived fragments and an octa-arginyl (R_8) peptide were synthesized by stepwise elongation techniques of Fmoc-protected amino acids on a Rink amide resin. Coupling reactions were performed using 5.0 equiv of Fmoc-protected amino acid, 5.0 equiv of diisopropylcarbodiimide and 5.0 equiv of 1-hydroxybenzotriazole monohydrate. Ac_2O–pyridine (1/1, v/v) for 20 min was used to acetylate the N-terminus of MA-derived fragments, with the exception of fragment 1. Chloroactylation of the N-terminus of the R_8 peptide, was achieved with 40 equiv of chloroacetic acid, 40 equiv of diisopropylcarbodiimide and 40 equiv of 1-hydroxybenzotriazole monohydrate, treated for 1 h. Cleavage of peptides from resin and side chain deprotection were carried out by stirring for 1.5 h with a mixture of TFA, thioanisole, ethanedithiol, *m*-cresol

* Corresponding authors. Tel.: +81 3 5285 1111; fax: +81 3 5285 5037 (T.M.); tel.: +81 3 5280 8036; fax: +81 3 5280 8039 (H.M.).
E-mail addresses: tmura@nih.go.jp (T. Murakami), tamamura.mr@tmd.ac.jp (H. Tamamura).

0968-0896/$ - see front matter © 2011 Elsevier Ltd. All rights reserved.
doi:10.1016/j.bmc.2011.12.055

and triisopropylsilane (8.15/0.75/0.75/0.25/0.25/0.1, v/v). After removal of the resins by filtration, the filtrate was concentrated under reduced pressure, and crude peptides were precipitated in cooled diethyl ether. All crude peptides were purified by RP-HPLC and identified by ESI-TOFMS. In the conjugation of the R_8 peptide (or iodoacetamide), the peptide (or iodoacetamide) solution in 0.1 M phosphate buffer, pH 7.8 was added to MA fragments which were synthesized as described above. The reaction mixture was stirred at room temperature under nitrogen. After 24 h (or 1 h for the conjugation of iodoacetamide), purification was performed by RP-HPLC. The purified peptides were identified by ESI-TOF MS and lyophilized. Purities of all final compounds were confirmed to be >95% by analytical HPLC. Detailed data are provided in Supplementary data.

2.2. Anti-HIV-1 assay

Anti-HIV-1 (NL4-3 or NL(AD8)) activity was determined by measurement of the protection against HIV-1-induced cytopathogenicity in MT-4 cells or PM1/CCR5 cells. Various concentrations of test peptide solutions were added to HIV-1 infected MT-4 or PM1/CCR5 cells at multiplicity of infection (MOI) of 0.001 and placed in wells of a 96-well microplate. After 5 day incubation at 37 °C in a CO_2 incubator, the number of viable cells was determined using the 3-(4,5-dimethylthiazol-2-yl)-2,5-diphenyltetrazolium bromide (MTT) method. The anti-HIV-1 (JR-CSF) activity was also determined by measuring capsid p24 antigen concentrations of the culture supernatant in the infected cultures by a commercially available ELISA assay (ZeptoMetrix Corp., Buffalo, NY).

2.3. CD spectroscopy

CD spectra were recorded on a JASCO J-720 spectropolarimeter at 25 °C. The measurements were performed using a 0.1 cm path length cuvette at a 0.1 nm spectral resolution. Each spectrum represents the average of 10 scans, and the scan rate was 50 nm/min. The concentrations of samples 8L and 9L were 28.2 and 64.7 μM, respectively, in PBS buffer (pH 7.4).

2.4. Fluorescent imaging of cell-penetrating MA peptides

Cells were seeded on 35 mm glass-bottom dish (2×10^5 cells/dish for HeLa and A549, 1×10^5 cells/dish for CHO-K1) one day before the experiments. The cells were cultured in DMEM/10% FBS/Penicillin–Streptomycin for HeLa and A549, or Ham's F12/10% FBS/Penicillin–Streptomycin for CHO-K1 at 37 °C/5% CO_2. Before the addition of MA peptides, cells were washed with Hanks' balanced salt solutions (HBSS) once. Peptides were added at 5 μM and further cultured for 30 min at 37 °C/5% CO_2. After incubation, cells were washed three times with HBSS and observed under a confocal laser-scanning microscopy (Zeiss LSM510).

3. Results and discussion

An overlapping peptide library spanning the whole sequence of the MA domain, p17, of NL4-3, the Gag precursor Pr55 of HIV-1 was designed. The full sequence of MA consists of 132 amino acid residues. In the peptide library, the MA sequence was divided from the N-terminus in 15-residue segments with an overlap of 5

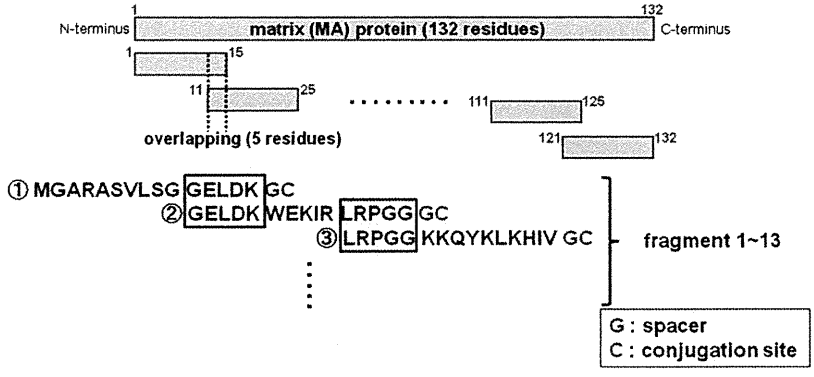

fragment number	sequence
1	H-MGARASVLSGGELDKGC-NH_2
2	CH_3CO-GELDKWEKIRLRPGGGC-NH_2
3	CH_3CO-LRPGGKKQYKLKHIVGC-NH_2
4	CH_3CO-LKHIVWASRELERFAGC-NH_2
5	CH_3CO-LERFAVNPGLLETSEGC-NH_2
6	CH_3CO-LETSEGSRQILGQLQGC-NH_2
7	CH_3CO-LGQLQPSLQTGSEELGC-NH_2
8	CH_3CO-GSEELRSLYNTIAVLGC-NH_2
9	CH_3CO-TIAVLYSVHQRIDVKGC-NH_2
10	CH_3CO-RIDVKDTKEALDKIEGC-NH_2
11	CH_3CO-LDKIEEEQNKSKKKAGC-NH_2
12	CH_3CO-SKKKAQQAAADTGNNGC-NH_2
13	CH_3CO-DTGNNSQVSQNYGC-NH_2

Figure 1. The construction of MA-based overlapping peptide library.

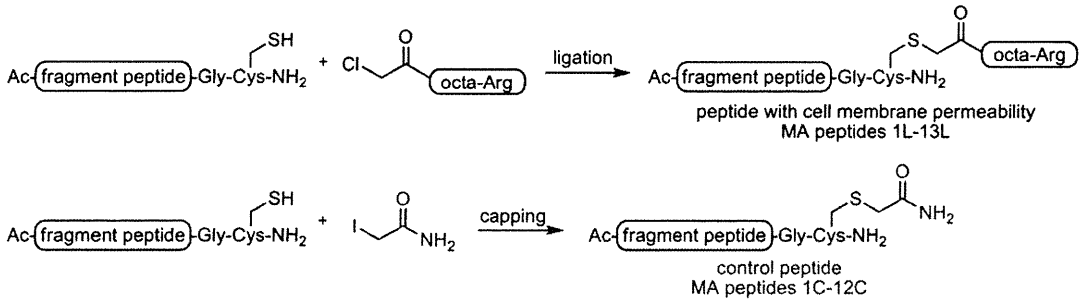

Figure 2. The design of MA peptides with cell membrane permeability (upper) and their control peptides (lower).

residues to preserve secondary structures (Fig. 1). Cys residues of the original MA sequence were changed into Ser residues because of the facility of peptide synthesis. Thirteen MA fragment peptides (1–13) were designed with the addition of Gly as a spacer and Cys as a conjugation site at the C-terminus. To impart cell membrane permeability to these peptides, the N-terminal chloroacetyl group of an octa-arginyl (R_8) peptide[19] was conjugated to the side-chain thiol group of the Cys residue of the above peptides. This resulted in the MA peptides 1L–13L (Fig. 2). R_8 is a cell membrane permeable motif and its fusion with parent peptides is known to produce bioactive peptides with no significant adverse properties.[12,13,20–24] In addition, the R_8-fusion can increase the solubility of MA

Table 1
Anti-HIV activity and cytotoxicity of control MA peptides

MA peptide	MT-4 cell	PM1/CCR5 cell		MT-4 cell
	NL4-3 (MTT assay) EC_{50}[a] (μM)	NL(AD8) (MTT assay) EC_{50}[a] (μM)	JR-CSF (p24 ELISA) EC_{50}[a] (μM)	(MTT assay) CC_{50}[b] (μM)
1C	>50	ND	ND	>50
2C	17 ± 1.4	1.0	ND	>50
3C	>50	ND	ND	>50
4C	No inhibition at 12.5 μM	ND	ND	14
5C	>50	ND	ND	>50
6C	37 ± 12	24% inhibition at 6.25 μM	25% inhibition at 50 μM	>50
7C	>50	ND	ND	>50
8C	>50	ND	ND	>50
9C	29 ± 1.4	13	8.1	>50
10C	No inhibition at 12.5 μM	ND	ND	17
11C	>50	ND	ND	>50
12C	>50	ND	ND	>50
14C	>50	ND	ND	>50
AZT	0.020	0.459	0.17	>100
SCH-D	ND	0.026	0.0014	ND

X4-HIV-1 (NL4-3 strain)-induced cytopathogenicity in MT-4 cells and R5-HIV-1 (NL(AD8) strain)-induced cytopathogenicity in PM1/CCR5 cells evaluated by the MTT assay, and inhibitory activity against R5-HIV-1 (JR-CSF strain)-induced cytopathogenicity in PM1/CCR5 cells evaluated by the p24 ELISA assay.

[a] EC_{50} values are the concentrations for 50% protection from HIV-1-induced cytopathogenicity in MT-4 cells.

[b] CC_{50} values are the concentrations for 50% reduction of the viability of MT-4 cells. All data are the mean values from at least three independent experiments. ND: not determined.

Table 2
Anti-HIV activity and cytotoxicity of MA peptides with cell membrane permeability

MA peptide	MT-4 cell	PM1/CCR5 cell		MT-4 cell
	NL4-3(MTT assay) EC_{50} (μM)	NL(AD8)(MTT assay) EC_{50} (μM)	JR-CSF(p24 ELISA) EC_{50} (μM)	(MTT assay) CC_{50} (μM)
1L	30	30	40	>50
2L	21 ± 4.2	>31	ND	32 ± 4.2
3L	no inhibition at 25 μM	ND	ND	36
4L	no inhibition at 3.13 μM	ND	ND	3.7
5L	40	42% inhibition at 50 μM	42	>50
6L	40 ± 8.9	49% inhibition at 50 μM	31	>50
7L	35 ± 1.5	37% inhibition at 50 μM	35% inhibition at 50 μM	>50
8L	2.3 ± 0.3	5.8	7.8	9.0 ± 2.4
9L	2.1 ± 0.5	0.43	0.58	5.7 ± 2.1
10L	43 ± 8.5	42% inhibitionat 50 μM	27	>50
11L	18 ± 3.0	17% inhibition at 25 μM	23	>50
12L	41 ± 5.5	30% inhibition at 25 μM	27	>50
13L	20 ± 2.1	0.43	11	>50
14L	no inhibition at 25 μM	ND	ND	36
AZT	0.020	0.459	0.17	>100
SCH-D	ND	0.026	0.0014	ND

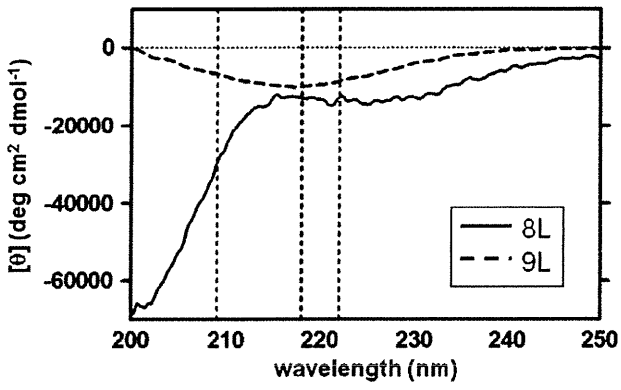

Figure 3. CD spectra of MA peptides 8L (28 μM) and 9L (65 μM) in PBS buffer, pH 7.4 at 25 °C.

peptides whose hydrophobicity is relatively limited. On the other hand, to develop control peptides lacking cell membrane permeability, iodoacetamide was conjugated to the thiol group of the Cys residue to prepare MA peptides 1C–12C (Fig. 2). MA peptide 13C was not synthesized because MA fragment 13 is insoluble in PBS buffer.

The anti-HIV activity of MA peptides 1L–13L and MA peptides 1C–12C, was evaluated. Inhibitory activity against T-cell line-tropic (X4-) HIV-1 (NL4-3 strain)-induced cytopathogenicity in MT-4 cells and against macrophage-tropic (R5-) HIV-1 (NL(AD8) strain)-induced cytopathogenicity in PM1/CCR5 cells was assessed by the 3-[4,5-dimethylthiazol-2-yl]-2,5-diphenyltetrazolium bromide (MTT) assay, and inhibitory activity against R5-HIV-1 (JR-CSF strain) replication in PM1/CCR5 cells was determined by the p24 ELISA assay. The results are shown in Tables 1 and 2. The control MA peptides 6C and 9C showed slight anti-HIV activity against NL4-3, NL(AD8) and JR-CSF strains, and 2C showed high anti-HIV activity against NL4-3 and NL(AD8) strains, but the other control MA peptides showed no significant anti-HIV activity. 2C showed significant anti-HIV activity against both X4-HIV-1 and R5-HIV-1 strains, suggesting that this region of the MA domain is relevant with Gag localization to the plasma membrane (PM)[25] and that 2C might inhibit competitively the interaction between MA and PM. On the other hand, the MA peptides with the exception of 3L and 4L, showed moderate to potent anti-HIV activity against all three strains. These peptides expressed almost the same level of anti-HIV activity against both X4-HIV-1 and R5-HIV-1 strains. The MA peptides 8L and 9L in particular, showed significant anti-HIV activity. These results suggest that MA peptides achieve entry into target cells as a result of the addition of R_8, and inhibit viral replication within the cells. The adjacent peptides 8L and 9L possess an overlapping sequence TIAVL. Such peptides exhibited relatively high cytotoxicity and the MA peptide 4L showed the highest cytotoxicity although it did not show any significant anti-HIV activity. The control MA peptides 1C–12C were relatively weakly cytotoxic. The MA peptides 8C and 9C exhibited no significant cytotoxicity, although the addition of R_8, giving 8L and 9L, caused a remarkable increase in cytotoxicity. This suggests that the octa-arginyl (R_8) sequence is correlated with the

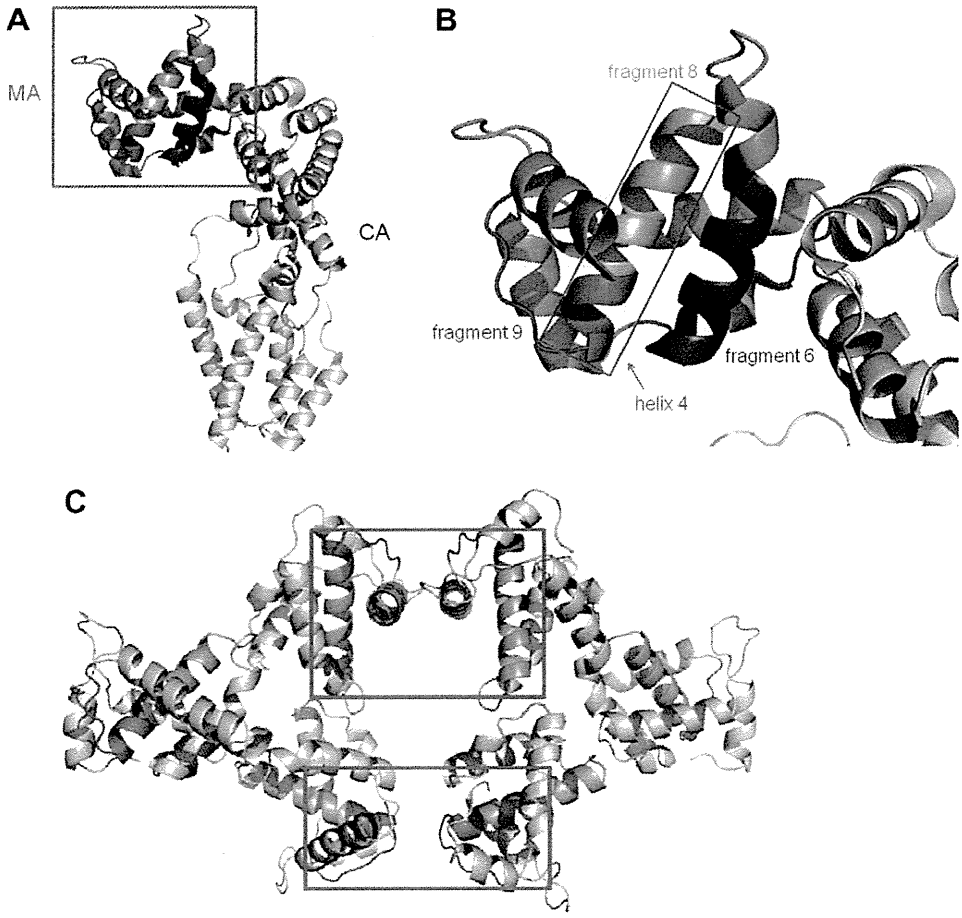

Figure 4. (A) The complete structure of MA and CA proteins (PDB ID: 2gol). (B) The enlarged structure of the highlighted region of (A). (C) The structure of an MA hexamer. Red-colored squares show interfaces between two MA trimers (PDB ID: 1hiw). Orange- and pink-colored helical ribbons represent fragments 8 and 9, respectively.

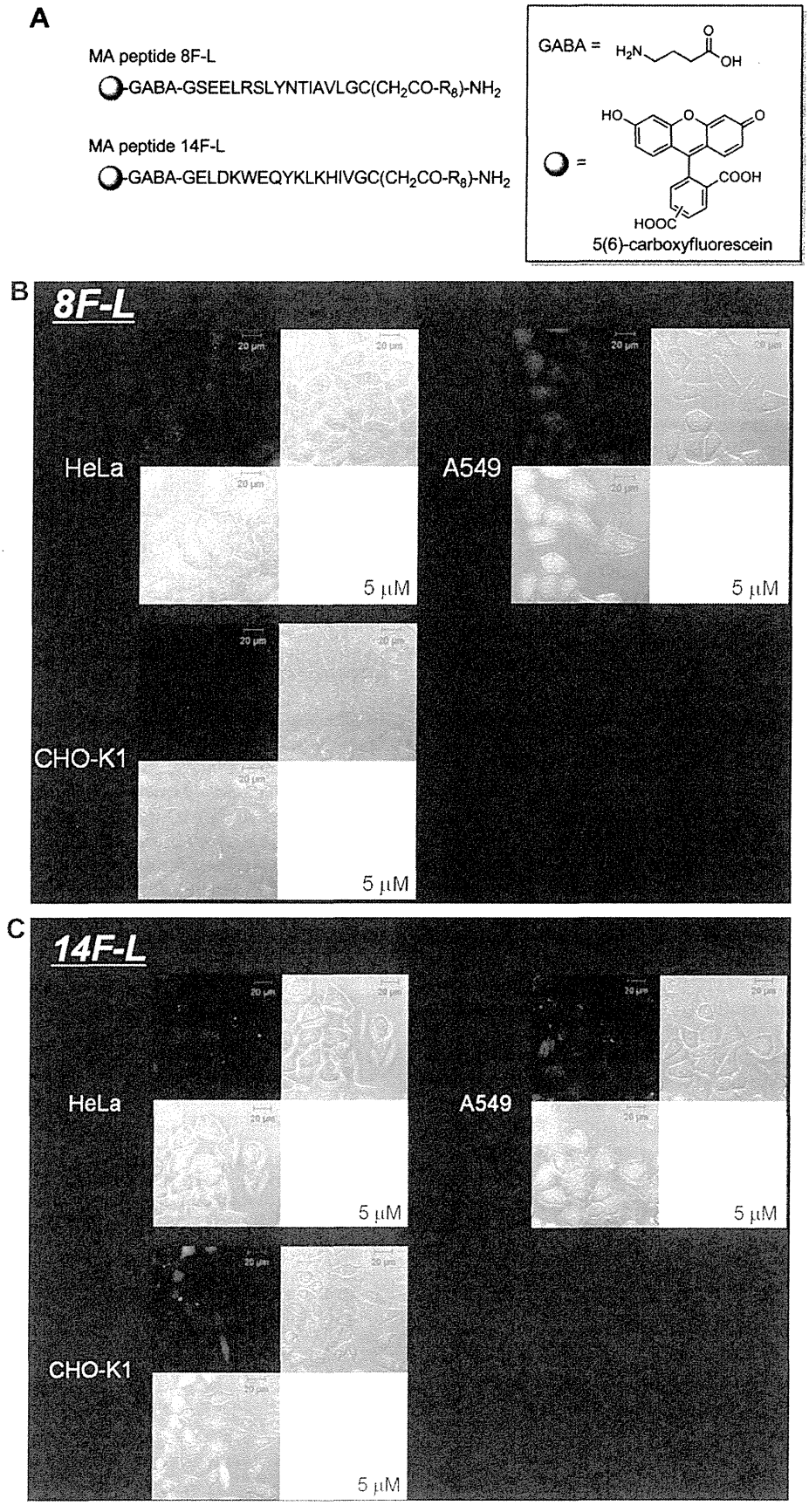

Figure 5. (A) The structures of fluorophore-labeled MA peptides 8F-L and 14F-L. (B) The fluorescent imaging of live cells HeLa, A549 and CHO-K1 by 8F-L. (C) The fluorescent imaging of live cells HeLa, A549 and CHO-K1 by 14F-L.

expression of cytotoxicity and in future, a different effective strategy for cell penetration may be advisable.

In the present assay, the control MA peptides 6C and 9C, which cover MA(51–65) and MA(81–95), respectively, showed significant anti-HIV activity. This is consistent with the previous studies, in which MA(41–55), MA(47–59) and MA(71–85) showed anti-HIV or dimerization inhibitory activity as discussed above.[16–18] These peptides have no R_8 sequence and thus cannot penetrate cell membranes. They exhibit inhibitory activity on the surface of cells, not intracellularly.

The structures of MA peptides 8L and 9L, dissolved in PBS buffer (2.7 mM KCl, 137 mM NaCl, 1.47 mM KH_2PO_4, 9.59 mM Na_2HPO_4) at pH 7.4, were determined by CD spectroscopy (Fig. 3). When peptides form α-helical structures, minima can be observed at approximately 207 and 222 nm in their CD spectra. The amino acid residues covering fragments 8 and 9 corresponding to 8L and 9L are located in an α-helical region (helix 4) of the parent MA protein (Fig. 4), and peptides 8L and 9L were presumed to have an α-helical conformation.[26–28] However, the CD spectra shown in Figure 3, suggest that these peptides lack any characteristic secondary structure. This is because the 15-mer peptide derived from MA is not sufficiently long to form a secondary structure even though Gly, Cys and octa-Arg are attached to their C-terminus. Analysis of the CD spectra suggests MA fragment peptides need a longer sequence in order to form a secondary structure. The CD spectra of the control MA peptides 8C and 9C were not determined because the aqueous solubility of these peptides is inadequate.

Fluorescent imaging of live cells was used to evaluate the cell membrane permeability of the MA peptides 8L and 14L, which showed high and zero significant anti-HIV activity, respectively. The MA fragment 14 is a hybrid of the fragments 2 and 3, and the MA peptides 14L and 14C, which are based on the conjugation of the N-terminal chloroacetyl group of an R_8 peptide and iodoacetamide to the thiol group of the Cys residue, respectively (Supplementary data), are control peptides lacking significant anti-HIV activity (Tables 1 and 2). These peptides were labeled with 5(6)-carboxyfluorescein via a GABA linker at the N-terminus to produce 8F–L and 14F–L (Fig. 5A). The fluorophore-labeled peptides 8F–L and 14F–L were incubated with live cells of HeLa, A549 and CHO-K1, and the imaging was analyzed by a fluorescence microscope (Fig. 5B and C). A549 cells are human lung adenocarcinomic human alveolar basal epithelial cells.[29] Similar penetration of both peptides 8F–L and 14F–L into these cells was observed. Even peptides without significant anti-HIV activity can penetrate cell membranes. The penetration efficiency of both peptides into A549 was relatively high and into HeLa was low. In CHO-K1 the penetration efficiency of 8F–L is relatively low, but that of 14F–L is high. These imaging data confirm that the MA peptides with the R_8 sequence can penetrate cell membranes and suggest that MA peptides such as 8L and 9L should be able to inhibit HIV replication inside cells.

4. Conclusions

Several HIV-1 inhibitory fragment peptides were identified through the screening of an overlapping peptide library derived from the MA protein. Judging by the imaging experiments, peptides possessing the R_8 group can penetrate cell membranes and might exhibit their function intracellularly thus inhibiting HIV replication.

Two possible explanations for the inhibitory activity of these MA fragment peptides can be envisaged: (1) The fragment peptides might attack an MA protein and inhibit the assembly of MA proteins. (2) These peptides might attack a cellular protein and inhibit its interaction with MA. Further studies to elucidate detailed action mechanisms and identify the targets of these peptides will be performed in future. The technique of addition of the R_8 group to peptides enabled us to screen library peptides that function within cells. Thus, the design of an overlapping peptide library of fragment peptides derived from a parent protein with a cell membrane permeable signal is a useful and efficient strategy for finding potent cell-penetrating lead compounds.

In the present study, the MA peptides 8L and 9L were shown to inhibit HIV-1 replication with submicromolar to micromolar EC_{50} values in cells using the MT-4 assay (NL4-3 and NL(AD8) strains) and the p24 ELISA assay (JR-CSF strain). Our findings suggest that these peptides could serve as lead compounds for the discovery of novel anti-HIV agents. Amino acid residues covering fragments 8 and 9 corresponding to 8L and 9L are located in the exterior surface of MA, and in particular in the interface between two MA trimers (Fig. 4C).[26–28] The interaction of two MA trimers leads to the formation of an MA hexamer, which is the MA assembly with physiological significance. Thus, the region covering fragments 8 and 9 is critical to oligomerization of MA proteins. This suggests that MA peptides 8L and 9L might inhibit the MA oligomerization through competitive binding to the parent MA, and that more potent peptides or peptidomimetic HIV inhibitors could result from studies on the mechanism of action of these MA peptides and identification of the interaction sites. Taken together, some seeds for anti-HIV agents are inherent in MA proteins, including inhibitors of the interaction with PM such as the MA peptide 2C.

Acknowledgements

This work was supported in part by Grant-in-Aid for Scientific Research from the Ministry of Education, Culture, Sports, Science, and Technology of Japan, and Health and Labour Sciences Research Grants from Japanese Ministry of Health, Labor, and Welfare. C.H. and T.T. were supported by JSPS Research Fellowships for Young Scientists. The authors thank Ms. M. Kawamata, National Institute of Infectious Diseases, for her assistance in the anti-HIV assay. We also thank Dr. Y. Maeda, Kumamoto University, for providing PM1/CCR5 cells, and Mr. S. Kumakura, Kureha Corporation, for providing SCH-D, respectively.

Supplementary data

Supplementary data associated with this article can be found, in the online version, at doi:10.1016/j.bmc.2011.12.055.

References and notes

1. Ghosh, A. K.; Dawson, Z. L.; Mitsuya, H. *Bioorg. Med. Chem.* **2007**, *15*, 7576.
2. Cahn, P.; Sued, O. *Lancet* **2007**, *369*, 1235.
3. Grinsztejn, B.; Nguyen, B.-Y.; Katlama, C.; Gatell, J. M.; Lazzarin, A.; Vittecoq, D.; Gonzalez, C. J.; Chen, J.; Harvey, C. M.; Isaacs, R. D. *Lancet* **2007**, *369*, 1261.
4. Tamamura, H.; Xu, Y.; Hattori, T.; Zhang, X.; Arakaki, R.; Kanbara, K.; Omagari, A.; Otaka, A.; Ibuka, T.; Yamamoto, N.; Nakashima, H.; Fujii, N. *Biochem. Biophys. Res. Commun.* **1998**, *253*, 877.
5. Fujii, N.; Oishi, S.; Hiramatsu, K.; Araki, T.; Ueda, S.; Tamamura, H.; Otaka, A.; Kusano, S.; Terakubo, S.; Nakashima, H.; Broach, J. A.; Trent, J. O.; Wang, Z.; Peiper, S. C. *Angew. Chem., Int. Ed.* **2003**, *42*, 3251.
6. Tamamura, H.; Hiramatsu, K.; Mizumoto, M.; Ueda, S.; Kusano, S.; Terakubo, S.; Akamatsu, M.; Yamamoto, N.; Trent, J. O.; Wang, Z.; Peiper, S. C.; Nakashima, H.; Otaka, A.; Fujii, N. *Org. Biomol. Chem.* **2003**, *1*, 3663.
7. Tanaka, T.; Nomura, W.; Narumi, T.; Masuda, A.; Tamamura, H. *J. Am. Chem. Soc.* **2010**, *132*, 15899.
8. Yamada, Y.; Ochiai, C.; Yoshimura, K.; Tanaka, T.; Ohashi, N.; Narumi, T.; Nomura, W.; Harada, S.; Matsushita, S.; Tamamura, H. *Bioorg. Med. Chem. Lett.* **2010**, *20*, 354.
9. Narumi, T.; Ochiai, C.; Yoshimura, K.; Harada, S.; Tanaka, T.; Nomura, W.; Arai, H.; Ozaki, T.; Ohashi, N.; Matsushita, S.; Tamamura, H. *Bioorg. Med. Chem. Lett.* **2010**, *20*, 5853.
10. Yoshimura, K.; Harada, S.; Shibata, J.; Hatada, M.; Yamada, Y.; Ochiai, C.; Tamamura, H.; Matsushita, S. *J. Virol.* **2010**, *84*, 7558.

11. Otaka, A.; Nakamura, M.; Nameki, D.; Kodama, E.; Uchiyama, S.; Nakamura, S.; Nakano, H.; Tamamura, H.; Kobayashi, Y.; Matsuoka, M.; Fujii, N. *Angew. Chem., Int. Ed.* **2002**, *41*, 2937.
12. Suzuki, S.; Urano, E.; Hashimoto, C.; Tsutsumi, H.; Nakahara, T.; Tanaka, T.; Nakanishi, Y.; Maddali, K.; Han, Y.; Hamatake, M.; Miyauchi, K.; Pommier, Y.; Beutler, J. A.; Sugiura, W.; Fuji, H.; Hoshino, T.; Itotani, K.; Nomura, W.; Narumi, T.; Yamamoto, N.; Komano, J. A. *J. Med. Chem.* **2010**, *53*, 5356.
13. Suzuki, S.; Maddali, K.; Hashimoto, C.; Urano, E.; Ohashi, N.; Tanaka, T.; Ozaki, T.; Arai, H.; Tsutsumi, H.; Narumi, T.; Nomura, W.; Yamamoto, N.; Pommier, Y.; Komano, J. A.; Tamamura, H. *Bioorg. Med. Chem.* **2010**, *18*, 6771.
14. Freed, E. O. *Virology* **1998**, *251*, 1.
15. Bukrinskaya, A. *Virus Res.* **2007**, *124*, 1.
16. Niedrig, M.; Gelderblom, H. R.; Pauli, G.; März, J.; Bickhard, H.; Wolf, H.; Modrow, S. *J. Gen. Virol.* **1994**, *75*, 1469.
17. Cannon, P. M.; Matthews, S.; Clark, N.; Byles, E. D.; Iourin, O.; Hockley, D. J.; Kingsman, S. M.; Kingsman, A. J. *J. Virol.* **1997**, *71*, 3474.
18. Morikawa, Y.; Kishi, T.; Zhang, W. H.; Nermut, M. V.; Hockley, D. J.; Jones, I. M. *J. Virol.* **1995**, *69*, 4519.
19. Suzuki, T.; Futaki, S.; Niwa, M.; Tanaka, S.; Ueda, K.; Sugiura, Y. *J. Biol. Chem.* **2002**, *277*, 2437.
20. Wender, P. A.; Mitchell, D. J.; Pattabiraman, K.; Pelkey, E. T.; Steinman, L.; Rothbard, J. B. *Proc. Natl. Acad. Sci. U.S.A.* **2000**, *97*, 13003.
21. Matsushita, M.; Tomizawa, K.; Moriwaki, A.; Li, S. T.; Terada, H.; Matsui, H. *J. Neurosci.* **2001**, *21*, 6000.
22. Takenobu, T.; Tomizawa, K.; Matsushita, M.; Li, S. T.; Moriwaki, A.; Lu, Y. F.; Matsui, H. *Mol. Cancer Ther.* **2002**, *1*, 1043.
23. Wu, H. Y.; Tomizawa, K.; Matsushita, M.; Lu, Y. F.; Li, S. T.; Matsui, H. *Neurosci. Res.* **2003**, *47*, 131.
24. Rothbard, J. B.; Garlington, S.; Lin, Q.; Kirschberg, T.; Kreider, E.; McGrane, P. L.; Wender, P. A.; Khavari, P. A. *Nat. Med.* **2000**, *6*, 1253.
25. Ono, A. *J. Virol.* **2004**, *78*, 1552.
26. Rao, Z.; Belyaev, A. S.; Fry, E.; Roy, P.; Jones, I. M.; Stuart, D. I. *Nature* **1995**, *378*, 743.
27. Hill, C. P.; Worthylake, D.; Bancroft, D. P.; Christensen, A. M.; Sundquist, W. I. *Proc. Natl. Acad. Sci. U.S.A.* **1996**, *93*, 3099.
28. Kelly, B. N.; Howard, B. R.; Wang, H.; Robinson, H.; Sundquist, W. I.; Hill, C. P. *Biochemistry* **2006**, *45*, 11257.
29. Murdoch, C.; Monk, P. N.; Finn, A. *Immunology* **1999**, *98*, 36.

frontiers in
MICROBIOLOGY

ORIGINAL RESEARCH ARTICLE
published: 14 May 2013
doi: 10.3389/fmicb.2013.00117

Increased infectivity in human cells and resistance to antibody-mediated neutralization by truncation of the SIV gp41 cytoplasmic tail

*Takeo Kuwata[1], Kaori Takaki[1], Ikumi Enomoto[1], Kazuhisa Yoshimura[2] and Shuzo Matsushita[1]**

[1] Center for AIDS Research, Kumamoto University, Kumamoto, Japan
[2] AIDS Research Center, National Institute of Infectious Diseases, Tokyo, Japan

Edited by:
Akio Adachi, The University of Tokushima Graduate School, Japan

Reviewed by:
Tetsuro Matano, University of Tokyo, Japan
Tsutomu Murakami, National Institute of Infectious Diseases, Japan
Hirofumi Akari, Kyoto University, Japan

***Correspondence:**
Shuzo Matsushita, Center for AIDS Research, Kumamoto University, 2-2-1 Honjo, Chuo-ku, Kumamoto 860-0811, Japan.
e-mail: shuzo@kumamoto-u.ac.jp

The role of antibodies in protecting the host from human immunodeficiency virus type 1 (HIV-1) infection is of considerable interest, particularly because the RV144 trial results suggest that antibodies contribute to protection. Although infection of non-human primates with simian immunodeficiency virus (SIV) is commonly used as an animal model of HIV-1 infection, the viral epitopes that elicit potent and broad neutralizing antibodies to SIV have not been identified. We isolated a monoclonal antibody (MAb) B404 that potently and broadly neutralizes various SIV strains. B404 targets a conformational epitope comprising the V3 and V4 loops of Env that intensely exposed when Env binds CD4. B404-resistant variants were obtained by passaging viruses in the presence of increasing concentration of B404 in PM1/CCR5 cells. Genetic analysis revealed that the Q733stop mutation, which truncates the cytoplasmic tail of gp41, was the first major substitution in Env during passage. The maximal inhibition by B404 and other MAbs were significantly decreased against a recombinant virus with a gp41 truncation compared with the parental SIVmac316. This indicates that the gp41 truncation was associated with resistance to antibody-mediated neutralization. The infectivities of the recombinant virus with the gp41 truncation were 7,900-, 1,000-, and 140-fold higher than those of SIVmac316 in PM1, PM1/CCR5, and TZM-bl cells, respectively. Immunoblotting analysis revealed that the gp41 truncation enhanced the incorporation of Env into virions. The effect of the gp41 truncation on infectivity was not obvious in the HSC-F macaque cell line, although the resistance of viruses harboring the gp41 truncation to neutralization was maintained. These results suggest that viruses with a truncated gp41 cytoplasmic tail were selected by increased infectivity in human cells and by acquiring resistance to neutralizing antibody.

Keywords: SIV, gp41, truncation, infectivity, resistance, neutralization, antibody

INTRODUCTION

The RV144 trial demonstrated 31% vaccine efficacy for preventing human immunodeficiency virus type 1 (HIV-1) infection (Rerks-Ngarm et al., 2009). Antibodies against the HIV-1, particularly against the V1/V2 loops, correlate inversely with infection risk (Haynes et al., 2012). Further recent isolation of monoclonal antibodies (MAbs) that neutralize a broad range of HIV-1 strains suggest the possibility for developing a vaccine that can induce cross-neutralizing antibodies effective for various HIV-1 strains (Kwong and Mascola, 2012). Although non-human primate models of simian immunodeficiency virus (SIV) infection can facilitate the evaluation of immunogens, epitopes and immune correlates, no potent and broad neutralizing MAb against SIV had been available.

To understand the mechanisms involved in neutralization of infectivity by antibodies in an SIV model, we recently isolated MAb B404 from a SIVsmH635FC-infected rhesus macaque, which potently and broadly neutralizes various SIV strains, such as SIVsmE543-3, SIVsmE660 and the neutralization-resistant variants, genetically diverse SIVmac316, and highly neutralization-resistant SIVmac239 (Kuwata et al., 2011). The B404 epitope, which comprises the V3 and V4 loops of Env and is intensely exposed by ligation of Env to CD4, is the target for potent and broad neutralization of SIV (Kuwata et al., 2013). Vigorous induction of B404-like neutralizing antibodies using the specific VH3 gene with a long complementarity-determining region 3 loop and λ light chain was observed in four SIVsmH635FC-infected macaques. The B404-resistant variants were induced by passaging viruses in the presence of increasing concentrations of B404. Genetical analysis of the gp120 region of B404-resistant variants revealed that the mutations in the C2 region of Env were important for the resistance to antibody-mediated neutralization (Kuwata et al., 2013).

In the present study, we further analyzed B404-resistant variants and determined the precise region responsible for the resistance to antibody-mediated neutralization. Genetic analysis of viruses during passage in the presence of B404 as well as phenotypic analysis using recombinant viruses revealed that a truncation of the gp41 cytoplasmic tail was the primary step leading to escape from neutralization.

MATERIALS AND METHODS

CELLS

PM1 (Lusso et al., 1995), PM1/CCR5 (Yusa et al., 2005), and HSC-F (Akari et al., 1999) cells were maintained in Roswell Park Memorial Institute (RPMI) 1640 medium containing 10% fetal bovine serum (FBS). TZM-bl (Platt et al., 1998; Derdeyn et al., 2000; Wei et al., 2002; Takeuchi et al., 2008) and 293T (DuBridge et al., 1987) cells were maintained in Dulbecco's modified Eagle's medium containing 10% FBS.

GENETIC ANALYSIS OF B404-RESISTANT VARIANTS

The induction of variants resistant to Fab-B404 (Kuwata et al., 2011) from SIVmac316 (Mori et al., 1992) harboring full-length gp41 was performed as described previously (Yoshimura et al., 2006; Hatada et al., 2010; Kuwata et al., 2013). Briefly, 5,000 $TCID_{50}$ (50% tissue culture infectious dose) SIVmac316 was incubated with 5 ng/ml Fab-B404 for 30 min at 37°C. Then, 5×10^4 PM1/CCR5 cells were added to the virus–Fab mixture. After incubation for 5 h, cells were washed with phosphate-buffered saline (PBS) and resuspended in RPMI 1640 supplemented with 10% FBS without Fab-B404. The culture supernatant was harvested 7 days later and used to infect fresh PM1/CCR5 cells for the next round of culture in the presence of increasing concentrations of Fab-B404. Proviral DNA samples were extracted from cells using a QIAamp DNA Blood Mini Kit (QIAGEN, Hilden, Germany) after 8, 17, 20, 23, and 26 passages as well as from P26C cells obtained after 26 passages in the absence of Fab-B404. The gp120 region was amplified using Platinum Taq DNA Polymerase High Fidelity (Invitrogen, Carlsbad, CA, USA) with primers SEnv-F (5′-ATG GGA TGT CTT GGG AAT CAG C-3′) and SER1 (5′-CCA AGA ACC CTA GCA CAA AGA CCC-3′). The whole *env* gene was amplified with primers SRev-F (5′-GGT TTG GGA ATA TGC TAT GAG-3′) and SEnv-R (5′-CCT ACT AAG TCA TCA TCT T-3′). The polymerase chain reaction (PCR) products were cloned using a TA cloning kit (Invitrogen), and subjected to sequencing. Nucleotide sequences were aligned and analyzed phylogenetically using Molecular Evolutionary Genetics Analysis version 5 (MEGA5) (Tamura et al., 2011).

CONSTRUCTION OF INFECTIOUS MOLECULAR CLONES WITH THE Env REGION FROM B404-RESISTANT VARIANTS

One of the clones from passage 26, P26B404 clone 26, was selected for construction of recombinant viruses, because this clone had mutations typical of the major population of P26B404 variants. Infectious molecular clones SS, SN, and NS were generated by replacing fragments *SphI–SacI* [nucleotides (nt) 6,446–9,226], *SphI–NheI* (nt 6,446–8,742), and *NheI–SacI* (nt 8,742–9,226) with the corresponding regions of SIVmac316, respectively. Mutants F277V and N295S, which have point mutations at amino acid residues 277 and 295 of Env, respectively, were constructed by PCR mutagenesis using the SIVmac316 plasmid as template. The changes from phenylalanine (TTC) to valine (GTC) in F277V and asparagine (AAT) to serine (AGT) in N295S were introduced using primers F277VFw (5′-TTG GTT TGG CGT CAA TGG TAC TAG GGC-3′), F277VRv (5′-GTA CCA TTG ACG CCA AAC CAA G-3′), N295SFw (5′-GGC AAT AGT AGT AGA ACC ATA ATT AG-3′), and N295SRv (5′-AAT TAT GGT TCT ACT ACT ATT GCC-3′). Mutant and parental SIVmac316 plasmids were transfected into 293T cells using X-tremeGENE 9 DNA Transfection Reagent (Roche Molecular Biochemicals, Mannheim, Germany). After 2 days, the supernatants containing viruses were filtered (0.45 μm) and stored at −80°C.

ANALYSIS OF VIRAL INFECTIVITY

For determination of $TCID_{50}$ in PM1 and PM1/CCR5 cells, 5×10^4 cells in 50 μl were inoculated with 50 μl serially diluted virus stocks in a 96-well plate and cultured for 2 weeks. Virus replication was judged by observation of cytopathic effects (CPE) by light microscopy. The $TCID_{50}$ in TZM-bl cells was determined by measuring luciferase activities. Briefly, 100 μl medium, 50 μl serially diluted virus stock, and 50 μl 1×10^4 cells containing 37.5 μg/ml diethylaminoethyl (DEAE) dextran were added to the wells of a 96-well plate. The plate was then incubated at 37°C for 2 days. After washing with PBS, cells were lysed with 30 μl cell lysing buffer (Promega, Madison, WI, USA) for 15 min at room temperature (RT) and then 10 μl of cell lysate was transferred to a 96-well white solid plate (Coster, Cambridge, MA, USA). Luciferase activity was measured using a Centro XS3 LB960 microplate luminometer (Berthold Technologies, Bad Wildbad, Germany) and a luciferase assay system (Promega). The $TCID_{50}$ was calculated according to the formula of Reed and Muench (1938).

Infectivity of viruses in PM1, PM1/CCR5, and HSC-F cells was evaluated by detecting infected cells using flow cytometry as described previously (Kuwata et al., 2011). Briefly, PM1 and PM1/CCR5 cells were adjusted to 1×10^6 cells/ml and HSC-F cells were adjusted to 5×10^6 cells/ml. Aliquots of 100 μl cells per well in a 24-well plate were inoculated with 100 μl of diluted virus stocks. After incubation for 6 h, 800 μl fresh medium was added to wells. One-half of the cells in each well were collected at 4, 7, and 10 days post-inoculation. Cells were washed with PBS and fixed with IC Fixation Buffer (eBioscience, San Diego, CA, USA). After washing with Permeabilization Buffer (eBioscience) twice, the cells were intracellularly stained with 4 μg/ml (50 μl) anti-p27 Fab, B450 (Kuwata et al., 2011) by incubation for 20 min at RT. The cells were then incubated with 50 μl anti-HA antibody (1:200; 3F10, Roche Molecular Biochemicals) for 20 min at RT followed by incubation with 50 μl of anti-rat-FITC (1:500; Santa Cruz Biotechnology, Santa Cruz, CA, USA) for 20 min at RT. The stained cells were analyzed using a FACSCalibur (BD Biosciences, Franklin Lakes, NJ, USA). Frequencies of infected cells were determined by comparison with an uninfected control. Data analysis was performed using FlowJo (TreeStar, San Carlos, CA, USA).

All infectivity experiments were performed at least twice and the representative results are shown.

ANALYSIS OF NEUTRALIZING ACTIVITIES

The Fab clones B404 and K8, isolated from an SIV-infected macaque (Kuwata et al., 2011), and murine MAb M318T (Matsumi et al., 1995) were used to examine the sensitivity of viruses to antibody-mediated neutralization in TZM-bl cells as described previously (Kuwata et al., 2011). Briefly, 100 μl serially diluted antibodies in duplicate were incubated with 200 $TCID_{50}$ (50 μl) of virus in a 96-well plate. After incubation for 1 h at 37°C, 100 μl

of 1×10^5 TZM-bl cells/ml containing 37.5 μg/ml DEAE dextran were added. After incubation for 2 days, luciferase activities were measured as described above for the analysis of viral infectivity. The 50% inhibitory concentrations (IC_{50}) and maximal percent of inhibition (MPI) were calculated from the average values by nonlinear regression using Prism5 (GraphPad Software, San Diego, CA, USA).

Sensitivity to neutralization by B404 in macaque cells was analyzed using HSC-F cells, a cynomolgus macaque cell line immortalized by infection with *Herpesvirus saimiri* (Akari et al., 1999). Fab-B404 was serially diluted and 50 μl aliquots were mixed with 50 μl undiluted or 10-fold diluted virus in a 96-well plate. After 1 h incubation at 37°C, 2×10^5 cells in 100 μl were added to each well and cultured for 1 day. The infected cells were washed twice with PBS, resuspended in 200 μl fresh medium, and cultured in a new 96-well plate. Viral infection was examined 4 days post-inoculation by intracellular staining of p27, as described above for the analysis of viral infectivity. Infectivity was determined in duplicate and the average value was used for the analysis of neutralization.

All neutralizing assays were performed at least twice and the representative results are shown.

WESTERN BLOTTING ANALYSIS OF VIRAL PROTEINS

Cells and supernatants were collected from six-well plate 2 days after transfection of 293T cells with infectious molecular clones, as previously described (Yuste et al., 2005). Supernatants were filtered (0.45 μm) and clarified by centrifugation for 10 min at 3,000 rpm. The clarified supernatants were centrifuged at 13,200 rpm for 90 min at 4°C, and the viral pellets were resuspended in 1 ml PBS and centrifuged again. Pellets were then dissolved in 80 μl sample buffer [62.5 mM Tris–HCl, pH 6.8, 2% sodium dodecyl sulfate (SDS), 25% glycerol, 5% 2-mercaptoethanol, 0.01% bromophenol blue]. Cells were washed with PBS and lysed in 300 μl sample buffer. Samples of virions and cell lysates were boiled for 5 min, and the proteins were separated by SDS-polyacrylamide gel electrophoresis using SuperSep Ace 5–20% (Wako Pure Chemical Industries, Osaka, Japan). Proteins were transferred to an Immun-Blot PVDF Membrane (Bio-Rad Laboratories, Hercules, CA, USA). The membrane was blocked with 5% skim milk TBS-T (Tris-buffered saline containing 0.1% Tween 20) for 1 h at RT, and then washed three times with TBS-T. For the detection of gp120, the membrane was incubated overnight at 4°C with 1 μg/ml M318T (Matsumi et al., 1995) in 5% skim milk TBS-T. After washing three times with TBS-T, the membrane was incubated with anti-mouse immunoglobulin G (IgG) peroxidase (1:4,000, Santa Cruz Biotechnology) for 1 h at RT. The membrane was washed three times with TBS-T and once with TBS, and then TMB solution (KPL, Gaithersburg, MD, USA) was added to develop color. Viral proteins gp41 and p26 were similarly examined using crude supernatants from bacterial culture producing B408 and B450 (Kuwata et al., 2011), which were mixed with the same amount of 5% skim milk TBS-T. The membrane was incubated with anti-HA-HRP antibody (1:1,000; Roche Molecular Biochemicals) and Chemi-Lumi One L (Nacalai Tesque, Kyoto, Japan), and viral proteins were visualized using ImageQuant LAS 4000 (GE Healthcare, Piscataway, NJ, USA)

RESULTS

EVOLUTION OF VIRUSES DURING PASSAGE UNDER THE PRESSURE OF Fab-B404

To select for variants resistant to MAb B404, an antibody that targets a conformational epitope comprising the gp120 V3 and V4 loops, we passaged SIVmac316 that possesses a full-length gp41 in PM1/CCR5 cells in the presence of increasing concentrations of Fab-B404. The virus recovered at passage 26 (P26B404) was resistant to neutralization by B404 (V3/V4) and other antibodies, MAbs K8 (CD4i) and M318T (V2), that target epitopes other than that recognized by B404 (Kuwata et al., 2013). The region covering the whole *env* gene were amplified by PCR and cloned from viruses at passage 8, 17, 20, 23, and 26. The nucleotide sequences were phylogenetically analyzed to show the evolution of B404-resistant variants (**Figure 1**). The first major mutation was a change from glutamine (CAG) to a stop codon (TAG) at 733rd amino acid residue of Env. The Q733stop substitution in the gp41 cytoplasmic domain was observed in 12 of 14 clones at passage 8 and in all clones thereafter. Another stop codon (W782stop) was the second

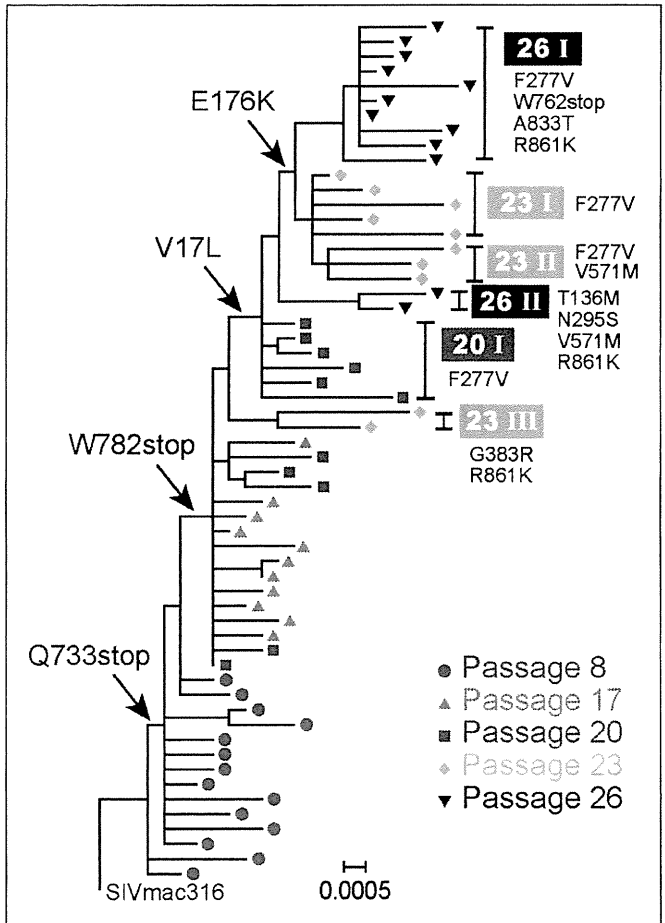

FIGURE 1 | Evolution of B404-resistant variants. Nucleotide sequences of the *env* gene, which were derived from proviruses at passages 8, 17, 20, 23, and 26, were phylogenetically analyzed using MEGA5. Arrows indicate major substitutions as follows: Q733stop, W782stop, V17L, and E176K. Clones with representative amino acid substitutions were separated into groups, which are shown on the right side along with the corresponding substitutions.

major mutation, which was detected after 17 passages. Substitutions V17L in the signal peptide and E176K in the V2 loop emerged after 20 and 23 passages, respectively, although the E176K substitution was also observed in P26C, control viruses after 26 passages in the absence of B404 (**Table 1**). In addition to these substitutions, most of clones acquired the F277V substitution in the late stage of evolution, except for one group at passage 26 which has the N295S substitution (see **Figure 1**, group 26II). Group 26II was clearly distinguished from group 26I by amino acid substitutions, such as T136M, N295S, and D571M/E (**Table 1**), suggesting two lineages of variants in P26B404.

These results demonstrated that the first step in acquiring resistance to B404 was the truncation of gp41. Although substitutions in gp120, represented by F277V, might contribute to the resistance to a high concentration of B404, 20 passages were required for the emergence of these substitutions.

Table 1 | Frequency* of amino acid substitutions in Env clones from B404-resistant variants after 26 passages.

Substitution	Region	P26B404		P26C
		I	II	
	gp120	**(*n* = 22)**	**(*n* = 8)**	**(*n* = 14)**
V17L	Signal peptide	**100%**	**100%**	0.0%
G62S	C1	0.0%	0.0%	21.4%
M67V/L/T	C1	4.5%	0.0%	21.4%
A68T	C1	0.0%	0.0%	**92.9%**
T136M	V1	4.5%	**87.5%**	0.0%
T137I	V1	0.0%	0.0%	14.3%
K141E/R	V1	0.0%	12.5%	7.1%
E176K	V2	**90.9%**	12.5%	35.7%
F277V	C2	**100%**	0.0%	0.0%
N295S	C2	0.0%	**100%**	0.0%
Q341H	V3	13.6%	12.5%	14.3%
D374N	C3	0.0%	0.0%	28.6%
K403R	V4	0.0%	12.5%	7.1%
W441R	C4	4.5%	0.0%	7.1%
	gp41	**(*n* = 10)**	**(*n* = 2)**	**(*n* = 7)**
F528S/L	Extracellular	20.0%	0.0%	0.0%
D571M/E	Extracellular	10.0%	**100%**	0.0%
Q733stop	Cytoplasmic	**100%**	**100%**	0.0%
W762stop	Cytoplasmic	**100%**	0.0%	0.0%
W782stop	Cytoplasmic	**100%**	0.0%	0.0%
A833T	Cytoplasmic	**90.0%**	0.0%	0.0%
R839K	Cytoplasmic	0.0%	0.0%	**57.1%**
R861K	Cytoplasmic	**100%**	**100%**	0.0%

Percentages of substitutions in populations P26B404 and P26C, which were obtained after 26 passages in the presence and absence of B404, respectively, are shown. The P26B404 population is separated into two subpopulations according to the phylogenetic analysis in **Figure 1. All the substitutions that are observed in more than one clone are shown here. Boldface indicates substitutions dominant (>50%) in each population. The numbers of clones analyzed for the gp120 and gp41 regions are shown in parentheses.*

TRUNCATION OF gp41 CONFERRED RESISTANCE TO ANTIBODY-MEDIATED NEUTRALIZATION

To analyze effect of substitutions in B404-resistant variants on resistance to neutralization, recombinant viruses were constructed (**Figure 2**). The *env* region of SIVmac316 was replaced by that of P26B404 clone 26, which had substitutions typical to the P26I group. The resultant molecular clones SS, SN, and NS had substitutions in the entire *env* region, gp120 and gp41 from P26B404I, respectively. SS and NS were predicted to have a truncated gp41 with no other mutation in gp41, because the Q733stop substitution was the first substitution in gp41. Point mutants with substitutions F277V and N295S, which were representative mutations at late passages, were also constructed by PCR mutagenesis.

These mutant viruses were examined for their sensitivity to neutralization by three MAbs B404 (V3/V4 conformational), K8 (CD4i), and M318T (V2). The neutralization of SS that contain the entire *env* region from P26B404I was similar to those of P26B404, indicating that the *env* region is responsible for the

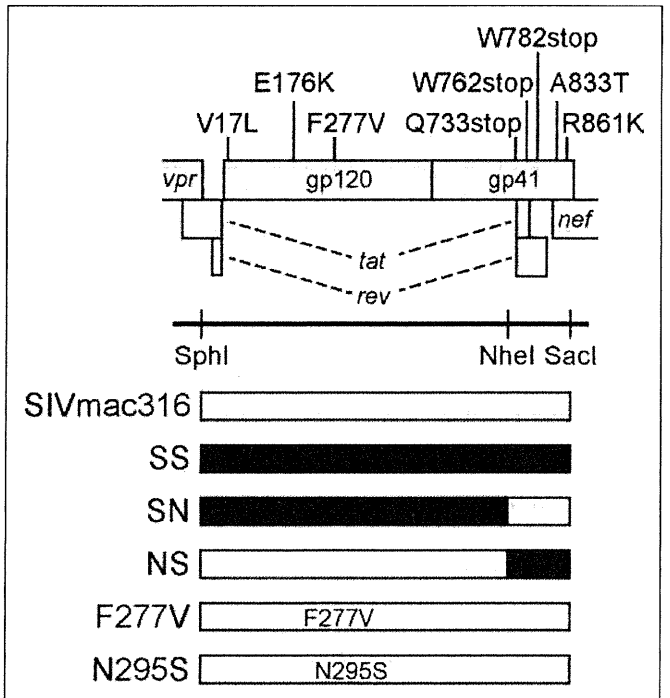

FIGURE 2 | Construction of infectious SIV clones with B404-resistant mutations. The open reading frames of the SIV genome are shown along with the Env substitutions in the B404-resistant variant typical to P26B404I. Full-length SIV clones were constructed from parental SIVmac316 by replacing the *env* region with that of the B404-resistant variant (blue) using *Sph*I, *Nhe*I, and *Sac*I sites. The resultant virus SS contains all of the Env substitutions present in P26B404I. Viruses SN and NS contain substitutions in gp120 and gp41, respectively. Point mutants F277V and N295S were constructed by inserting the substitutions F277V and N295S into SIVmac316, respectively.

resistance to neutralization (**Figure 3A**). Recombinants SN and NS, which have substitutions in gp120 and gp41 from P26B404I, respectively, showed varying degrees of resistance. The IC_{50} values of SN and NS against B404 were intermediates between the parental SIVmac316 and the neutralization-resistant P26B404. Maximal inhibition reached a plateau at 73.8, 82.3, and 81.9% in SS, NS, and P26B404, respectively, but the MPI value of SN (94.9%) was close to that of SIVmac316 (100%; **Figure 3B**). Neutralization resistance to anti-CD4i MAb K8 was characterized by decreases in the IC_{50} value of SN and the MPI of NS. Neutralization by anti-V2 MAb M318T was even enhanced in SN, although NS showed the resistance comparable to those of SS and P26B404. The decreases in MPI values were commonly observed for the neutralization of NS by the three MAbs (**Figure 3B**). Resistance to neutralization was not significantly detected by the point mutants F277V and N295S, except for the neutralization of F277V by K8 (4.3-fold decrease of IC_{50} value). These results indicated that the entire *env* region, including substitutions in both gp120 and gp41, was responsible for the full-resistance of P26B404 to neutralization. The decrease of MPI values for NS suggested that truncation of gp41 by the Q733stop substitution, the first major substitution in viral evolution, was important to escape from the neutralizing antibodies.

INCREASED INFECTIVITY FOR HUMAN CELLS BY SIV WITH A TRUNCATED gp41

Truncation of gp41 in SIV is associated with the adaptation to human cells (Hirsch et al., 1989; Kodama et al., 1989), which may partially contribute to neutralization resistance (Yuste et al., 2005). To explore the mechanism of neutralization resistance of P26B404, the infectivity of recombinant viruses was analyzed by determining the $TCID_{50}$ values of virus stocks prepared by transfection of 293T cells (**Table 2**). The $TCID_{50}$ values in all the human cells tested were significantly higher for SS and NS viruses with truncated gp41 than

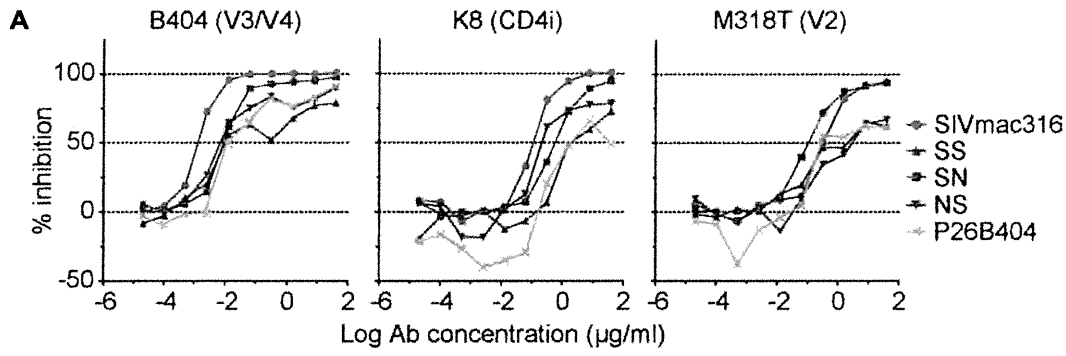

B

Neutralization profile of mutant viruses

Virus	B404 (V3/V4)		K8 (CD4i)		M318T (V2)	
	IC_{50}	MPI	IC_{50}	MPI	IC_{50}	MPI
SIVmac316	1.3E-03 (1.0)	100 (0.0)	1.1E-01 (1.0)	99.0 (0.0)	3.3E-01 (1.0)	94.3 (0.0)
SS	1.9E-02 (14.5)	73.8 (-26.2)	1.8E+00(16.3)	67.9 (-31.1)	9.4E-01 (2.8)	65.5 (-28.8)
SN	9.1E-03 (6.8)	94.9 (-5.1)	5.9E-01 (5.3)	94.7 (-4.4)	1.0E-01 (0.3)	92.5 (-1.8)
NS	6.8E-03 (5.1)	82.3 (-17.7)	2.1E-01 (1.9)	77.0 (-22.0)	1.7E+00 (5.2)	67.6 (-26.7)
F277V	3.8E-03 (2.8)	100 (0.0)	4.8E-01 (4.3)	99.6 (0.5)	3.0E-01 (0.9)	94.8 (0.5)
N295S	2.3E-03 (1.7)	99.6 (-0.4)	1.4E-01 (1.2)	99.9 (0.8)	3.1E-01 (0.9)	97.0 (2.7)
P26B404	1.7E-02 (12.5)	81.9 (-18.1)	8.2E-01 (7.3)	54.6 (-44.5)	2.5E-01 (0.8)	60.0 (-34.3)

Fold change of IC_{50}
> 10
3-10
< 3

% change of MPI
< -20
-10- to -20
> -10

FIGURE 3 | Sensitivities of viruses with B404-resistant mutations to neutralization by MAbs. (A) Sensitivities of mutant viruses SS, SN, and NS to neutralization by MAbs Fab-B404 (anti-V3/V4), Fab-K8 (anti-CD4i), and M318T (anti-V2) are shown. Neutralization of parental SIVmac316 and B404-resistant P26B404 is also shown as controls sensitive and resistant to neutralization, respectively. **(B)** The sensitivities to neutralization are represented by values for IC_{50} (μg/ml) and MPI (%). Viruses were examined for their sensitivities to neutralization by MAbs Fab-B404, Fab-K8, and M318T in TZM-bl cells. The IC_{50} and MPI values were determined using Prism 5. The fold-change of IC_{50} was calculated by dividing the IC_{50} value by that of the parental SIVmac316. Percent change of MPI was calculated by subtracting the MPI value from that of SIVmac316. These changes are shown in parentheses and significant changes are indicated by magenta (IC_{50}: >10; MPI: < −20) and orange (IC_{50}: 3–10; MPI: −20 to −10) highlighting.

parental SIVmac316 and SN, in which gp41 is intact. In particular, NS showed a striking increase in $TCID_{50}$ values, which were 7,100-, 1,000-, and 140-fold higher than those of parental SIVmac316 in PM1, PM1/CCR5, and TZM-bl cells, respectively. These results indicate that truncation of gp41 caused by the Q733stop substitution increases viral infectivity for human cells.

To compare viral infectivity in human and macaque cells, viral infection was monitored after inoculation of PM1 and PM1/CCR5 human cells and the HSC-F cynomolgus macaque cell line with varying dilutions of virus stocks (**Figure 4**). Consistent with the $TCID_{50}$ analysis, a higher frequency of infected cells was detected earlier in PM1 and PM1/CCR5 cells inoculated with NS than the parental SIVmac316. In contrast, SN showed decreased infectivity in PM1 and PM1/CCR5 cells, apparently because PM1 cells were not infected by a 1,000-fold diluted SN stock. Although the $TCID_{50}$ values of SS were much higher than those of SIVmac316, the replication kinetics of SS were similar to those of SIVmac316 in PM1 and PM1/CCR5 cells. These results suggest that gp41 truncation increases infectivity for human cells and that the substitutions in gp120 of P26B404I are associated with slow and poor replication compared with that of SIVmac316.

Infectivity for macaque cells was more significantly affected than that for human cells by the substitutions in gp120 of P26B404I (**Figure 4**, lower panels). Infected cells were detected in HSC-F cells inoculated with 1,000-fold diluted virus stocks of SIVmac316 and NS, but viral infection in HSC-F cells was limited to a low frequency even by inoculation with 10-fold diluted virus stocks of SS and SN. Truncation of gp41 did not significantly affect replication in HSC-F macaque cells, although truncation of gp41 was disadvantageous for replication in primary T cell cultures from macaques (Hirsch et al., 1989; Kodama et al., 1989).

These results demonstrate that gp41 truncation strikingly increases infectivity for human cells, but not for macaque cells, and that the substitutions in gp120 decrease infectivity in human and macaque cells. Truncation of gp41, which conferred extremely high infectivity for PM1/CCR5 cells, may be the first step to escape from neutralization and the substitutions in gp120 may be the second step to replicate in the presence of high concentration of B404.

Table 2 | Infectivity* of viruses with substitutions from P26B404.

Viruses	PM1	PM1/CCR5	TZM-bl
SIVmac316	4.2E+02 (1.0)	1.4E+03 (1.0)	9.6E+04 (1.0)
SS	2.9E+05 (710)	4.7E+05 (350)	6.3E+06 (66)
SN	2.0E+03 (4.8)	8.4E+03 (6.2)	2.9E+05 (3.1)
NS	2.9E+06 (7,100)	1.4E+06 (1,000)	1.4E+07 (140)

**Infectivity is shown by the $TCID_{50}$/ml values of the viruses, which were prepared by transfection of 293T cells, in PM1, PM1/CCR5, and TZM-bl cells. The fold-change, which was calculated by dividing the mutant $TCID_{50}$/ml value by that of the parental SIVmac316, is shown in the parentheses.*

INCREASED INCORPORATION OF Env INTO VIRIONS IN SIV WITH TRUNCATED gp41

Incorporation of Env into virions was examined using these recombinant viruses, because increased infectivity by gp41 truncation was suggested to be associated with the Env content of virions (Manrique et al., 2001; Zhu et al., 2003, 2006; Yuste et al., 2004, 2005). Analysis of viral proteins in cells and supernatants from transfected 293T cells revealed that incorporation of Env into virions was significantly high in SS and NS viruses with the Q733stop substitution (**Figure 5**). MAb to gp120 showed a higher amount

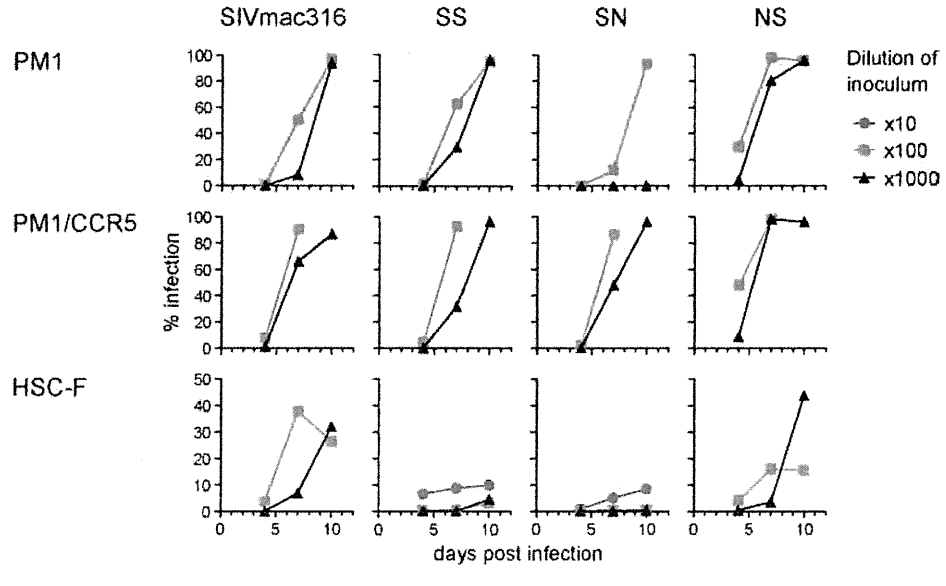

FIGURE 4 | Replication of B404-resistant viruses in human and macaque cells. Frequencies of infected cells at 4, 7, and 10 days post-infection are shown. PM1 and PM1/CCR5 human T cells and HSC-F cynomolgus macaque T cells were infected with the various dilutions of SIVmac316, SS, SN, and NS. Infected cells were detected using flow cytometry after intracellular staining by B450 (anti-p27 Fab).

of gp120 and gp160 in virions from SS and NS than those from SN and the parental SIVmac316, although the production of Env proteins in the transfected cells was at the same level among all the viruses (**Figure 5A**). MAb to gp41 also demonstrated that truncated gp41 was more abundant in virions compared with full-length gp41 (**Figure 5B**). Semi-quantification by densitometric scanning of gp41 and p26 images suggested that the levels of gp41 amount per virion in SS and NS were 12- and 44-fold higher than that of SIVmac316, respectively, after adjusting virion numbers using the p26 amounts. In contrast to the increased amount of Env proteins in virions from viruses with truncated gp41, the level of Gag p27 in virions was low in SS and NS compared with those in SN and SIVmac316 (**Figure 5C**). This indicates that the Env content per virion, which was normalized by the amount of p27, was significantly high in viruses with truncated gp41. These results suggest that truncation of gp41 by the Q733stop substitution enhances incorporation of Env into virions.

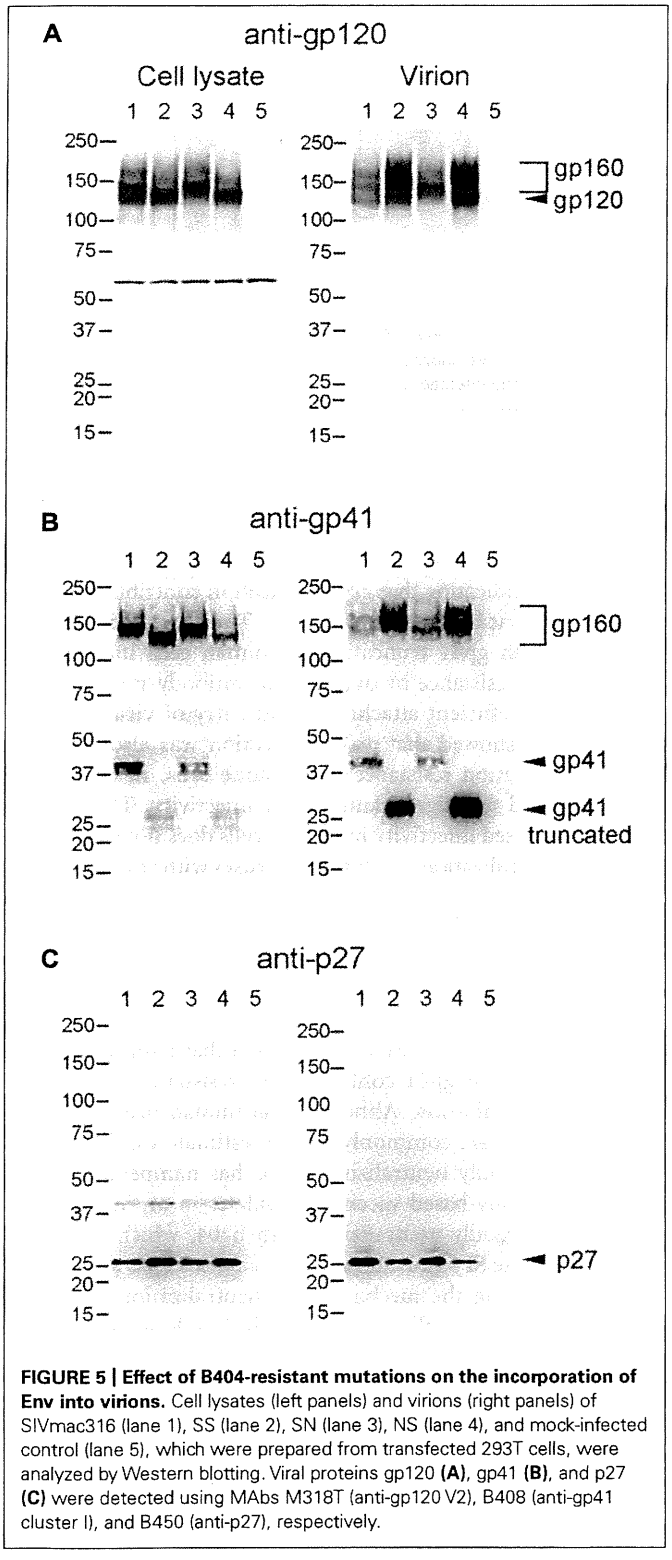

FIGURE 5 | Effect of B404-resistant mutations on the incorporation of Env into virions. Cell lysates (left panels) and virions (right panels) of SIVmac316 (lane 1), SS (lane 2), SN (lane 3), NS (lane 4), and mock-infected control (lane 5), which were prepared from transfected 293T cells, were analyzed by Western blotting. Viral proteins gp120 **(A)**, gp41 **(B)**, and p27 **(C)** were detected using MAbs M318T (anti-gp120 V2), B408 (anti-gp41 cluster I), and B450 (anti-p27), respectively.

NEUTRALIZATION RESISTANCE OF SIV WITH TRUNCATED gp41 IN MACAQUE CELLS

The analysis of infectivity of recombinant viruses suggested that the resistance to neutralization by truncation of gp41 might be due to adaptation to human cells. To examine this hypothesis, sensitivity to neutralization by B404 was determined in HSC-F macaque cells using SIVmac316 and NS, which showed similar infectivity for HSC-F cells (**Figure 4**). In flow cytometric analysis, infection in the presence or absence of B404 demonstrated that the high sensitivity of SIVmac316 and resistance of NS to neutralization were maintained in HSC-F cells (**Figure 6**). The frequency of infected cells decreased from 41.5% to the background level (2.03%) in inoculation with the undiluted stock of SIVmac316. In contrast, infection with NS, even with a 10-fold diluted virus stock, was significant in HSC-F cells in the presence of B404 (**Figure 6A**). Neutralization of NS in HSC-F cells was characterized by a decrease in maximal inhibition (**Figure 6B**), which was also observed in TZM-bl cells (**Figure 3A**). The magnitude of resistance of NS to B404 was greater when infection was performed using the undiluted stock compared with the 10-fold diluted stock, raising the possibility that B404 did not inhibit infection with a high titer of viruses. However, the resistance of NS was shown by infection with a low titer of NS, in which the frequency of infected cells in the absence of B404 (23.8%) was lower than infection with undiluted SIVmac316 (41.5%). Further, immunoblotting analysis revealed that the amount of virions was higher in the virus stock of SIVmac316 than that of NS (**Figure 5**).

These results indicate that gp41 truncation by the Q733stop substitution contributes to neutralization resistance of viruses in macaque cells. This suggests that the resistance to neutralization by truncation of gp41 is not due to the adaptation to human cells. The Q733stop substitution, the first major mutation during passages in the presence of B404, might be selected because it facilitates adaptation of virus to human cells and imparts resistance to antibody.

DISCUSSION

In the present study, truncation of the cytoplasmic tail of gp41, which was caused by the Q733stop substitution in Env, was the first major mutation detected during passage of SIV in the presence of the neutralizing antibody B404. Analysis of recombinant viruses suggested that the gp41 truncation was selected by their resistance to neutralizing antibody, which was characterized by the decrease of maximal inhibition compared with viruses with intact gp41, and

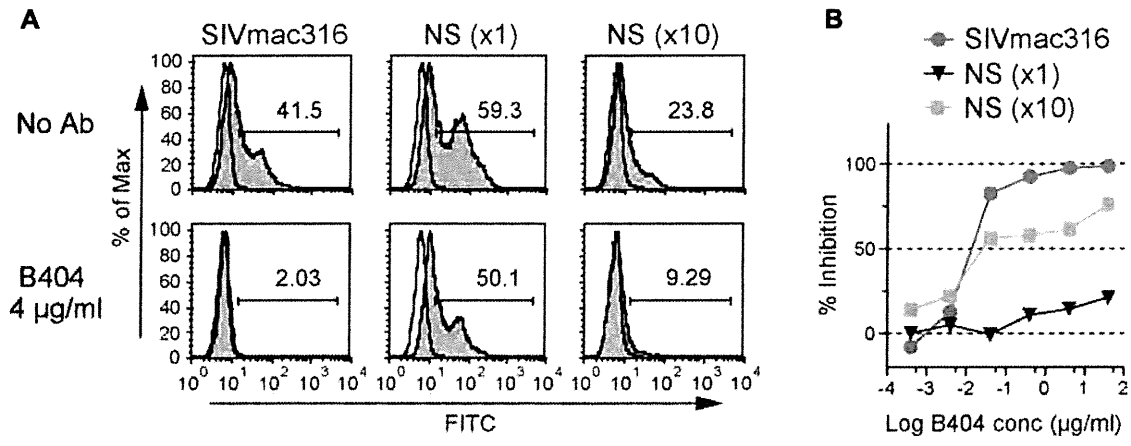

FIGURE 6 | Contribution of gp41 truncation to neutralization resistance in infection of macaque cells. (A) Infection of HSC-F cells in the presence (4 μg/ml) or absence of Fab-B404 is shown. HSC-F cells were inoculated with undiluted SIVmac316 and NS, and 10-fold diluted NS. Viral infection was monitored 4 days post-infection using flow cytometry after intracellular staining by B450 (anti-p27 Fab). **(B)** Neutralization of SIVmac316 and NS by B404 in HSC-F cells are shown. Percent inhibition was calculated by comparison with the infected culture in the absence of B404.

increased infectivity for human cells. The premature stop codon in the gp41 cytoplasmic region was frequently detected in SIV strains propagated in human cell culture *in vitro*, such as the original SIVmac316 clone, SIVmac1A11 and 17E-Fr (Hirsch et al., 1989; Kodama et al., 1989; Mori et al., 1992; Bonavia et al., 2005; Vzorov et al., 2005). The truncation of gp41 is considered as an adaptation of SIV to replication in human cell culture, because the premature stop codon rapidly reverted to express full-length gp41 after infection of rhesus primary cell culture *in vitro* and rhesus macaques *in vivo* (Hirsch et al., 1989; Kodama et al., 1989). Mutant viruses harboring the gp41 truncation showed increased infectivity for human cells, although the effects on infectivity varied depending on the SIV strain and the length of the gp41 truncation (Manrique et al., 2001; Yuste et al., 2004, 2005; Vzorov et al., 2005, 2007). The enhancement effect of gp41 truncation on incorporation of Env into virions, which were demonstrated by quantification of viral proteins in virions (Yuste et al., 2004) and electron tomography analysis of Env trimers on virions (Zhu et al., 2003, 2006), was partly associated with the increased infectivity caused by gp41 truncation (Manrique et al., 2001; Yuste et al., 2004, 2005). Because expression of Env on the cell surface is regulated by the cytoplasmic domain of gp41, truncation of gp41 may increase Env density on both cells and virions (LaBranche et al., 1995; Berlioz-Torrent et al., 1999; Postler and Desrosiers, 2013). Consistent with these studies, infectivity for human cells and Env incorporation into virions was enhanced by gp41 truncation in the present study. Although the mechanism responsible for increasing viral infectivity caused by gp41 truncation remains unclear, the high virion Env content may contribute to the efficient replication of viruses with truncated gp41 in human cells.

The effect of gp41 truncation on susceptibility to antibody-mediated neutralization is controversial, perhaps due to the SIV strains used for the analyses. Because most of prototypic SIV clones with truncated gp41 were macrophage-tropic, CD4-independent, and neutralization-sensitive (Mori et al., 1992; Bonavia et al., 2005; Vzorov et al., 2005), the truncation of gp41 was assumed responsible for the high sensitivity to neutralization. However, the resistance to neutralization by gp41 truncation was shown using the E767stop mutant of SIVmac316 (Yuste et al., 2005). This is consistent with our results using SIVmac316 harboring the Q733stop substitution, indicating that gp41 truncation contributes to resistance of SIVmac316 to neutralization. The increased infectivity of viruses with gp41 truncation in human cells may partially play a role in resistance by overcoming antibody-mediated neutralization via efficient attachment and entry of viruses to cells. However, we showed that gp41 truncation was also associated with neutralization resistance in macaque cells, in which gp41 truncation did not significantly affect infectivity. This suggests that the increased infectivity in human cells does not significantly affect the neutralization resistance of viruses with truncated gp41. As shown by provision of excess Env in trans, high Env content in virions may be critical for antibody-mediated neutralization (Yuste et al., 2005). Further studies will be required to understand the mechanism of resistance to neutralization conferred by gp41 truncation.

In the present study, we demonstrated that truncation of the cytoplasmic tail of gp41 contributes to resistance to antibody-mediated neutralization. Although non-human primate models of SIV infection are commonly used to estimate vaccine efficacy, the lack of broadly neutralizing MAbs has hampered development of antibody-based vaccine candidates in an SIV-macaque model. The broadly neutralizing MAb B404, which neutralizes multiple, diverse SIV isolates (Kuwata et al., 2013), is a useful tool for understanding the mechanism of neutralization in an SIV-macaque model and will contribute to the development of HIV-1 vaccines.

ACKNOWLEDGMENTS

We thank Dr. Hirofumi Akari for providing HSC-F cells. TZM-bl cells were obtained from Dr. John C. Kappes, Dr. Xiaoyun Wu, and Tranzyme Inc. through the NIH AIDS Research and Reference Reagent Program, Division of AIDS, NIAID, NIH. This work

was supported by MEXT KAKENHI Grant Number 10839786, the Program of Founding Research Centres for Emerging and Re-emerging Infectious Diseases, the Global COE program Global Education and Research Centre Aiming at the Control of AIDS and a grant-in-aid for scientific research (C-24591484) from the Ministry of Education, Culture, Sport, Science and Technology, Japan and a grant from the Ministry of Health, Welfare and Labour of Japan (H24-AIDS-007).

REFERENCES

Akari, H., Nam, K. H., Mori, K., Otani, I., Shibata, H., Adachi, A., et al. (1999). Effects of SIVmac infection on peripheral blood CD4+CD8+ T lymphocytes in cynomolgus macaques. *Clin. Immunol.* 91, 321–329.

Berlioz-Torrent, C., Shacklett, B. L., Erdtmann, L., Delamarre, L., Bouchaert, I., Sonigo, P., et al. (1999). Interactions of the cytoplasmic domains of human and simian retroviral transmembrane proteins with components of the clathrin adaptor complexes modulate intracellular and cell surface expression of envelope glycoproteins. *J. Virol.* 73, 1350–1361.

Bonavia, A., Bullock, B. T., Gisselman, K. M., Margulies, B. J., and Clements, J. E. (2005). A single amino acid change and truncated TM are sufficient for simian immunodeficiency virus to enter cells using CCR5 in a CD4-independent pathway. *Virology* 341, 12–23.

Derdeyn, C. A., Decker, J. M., Sfakianos, J. N., Wu, X., O'Brien, W. A., Ratner, L., et al. (2000). Sensitivity of human immunodeficiency virus type 1 to the fusion inhibitor T-20 is modulated by coreceptor specificity defined by the V3 loop of gp120. *J. Virol.* 74, 8358–8367.

DuBridge, R. B., Tang, P., Hsia, H. C., Leong, P. M., Miller, J. H., and Calos, M. P. (1987). Analysis of mutation in human cells by using an Epstein–Barr virus shuttle system. *Mol. Cell. Biol.* 7, 379–387.

Hatada, M., Yoshimura, K., Harada, S., Kawanami, Y., Shibata, J., and Matsushita, S. (2010). Human immunodeficiency virus type 1 evasion of a neutralizing anti-V3 antibody involves acquisition of a potential glycosylation site in V2. *J. Gen. Virol.* 91, 1335–1345.

Haynes, B. F., Gilbert, P. B., Mcelrath, M. J., Zolla-Pazner, S., Tomaras, G. D., Alam, S. M., et al. (2012). Immune-correlates analysis of an HIV-1 vaccine efficacy trial. *N. Engl. J. Med.* 366, 1275–1286.

Hirsch, V. M., Edmondson, P., Murphey-Corb, M., Arbeille, B., Johnson, P. R., and Mullins, J. I. (1989). SIV adaptation to human cells. *Nature* 341, 573–574.

Kodama, T., Wooley, D. P., Naidu, Y. M., Kestler, H. W. III, Daniel, M. D., Li, Y., et al. (1989). Significance of premature stop codons in env of simian immunodeficiency virus. *J. Virol.* 63, 4709–4714.

Kuwata, T., Katsumata, Y., Takaki, K., Miura, T., and Igarashi, T. (2011). Isolation of potent neutralizing monoclonal antibodies from an SIV-Infected rhesus macaque by phage display. *AIDS Res. Hum. Retroviruses* 27, 487–500.

Kuwata, T., Takaki, K., Yoshimura, K., Enomoto, I., Wu, F., Ourmanov, I., et al. (2013). Conformational epitope consisting of the V3 and V4 loops as a target for potent and broad neutralization of simian immunodeficiency viruses. *J. Virol.* 87, 5424–5436.

Kwong, P. D., and Mascola, J. R. (2012). Human antibodies that neutralize HIV-1: identification, structures, and B cell ontogenies. *Immunity* 37, 412–425.

LaBranche, C. C., Sauter, M. M., Haggarty, B. S., Vance, P. J., Romano, J., Hart, T. K., et al. (1995). A single amino acid change in the cytoplasmic domain of the simian immunodeficiency virus transmembrane molecule increases envelope glycoprotein expression on infected cells. *J. Virol.* 69, 5217–5227.

Lusso, P., Cocchi, F., Balotta, C., Markham, P. D., Louie, A., Farci, P., et al. (1995). Growth of macrophage-tropic and primary human immunodeficiency virus type 1 (HIV-1) isolates in a unique CD4+ T-cell clone (PM1): failure to downregulate CD4 and to interfere with cell-line-tropic HIV-1. *J. Virol.* 69, 3712–3720.

Manrique, J. M., Celma, C. C., Affranchino, J. L., Hunter, E., and Gonzalez, S. A. (2001). Small variations in the length of the cytoplasmic domain of the simian immunodeficiency virus transmembrane protein drastically affect envelope incorporation and virus entry. *AIDS Res. Hum. Retroviruses* 17, 1615–1624.

Matsumi, S., Matsushita, S., Yoshimura, K., Javaherian, K., and Takatsuki, K. (1995). Neutralizing monoclonal antibody against a external envelope glycoprotein (gp110) of SIVmac251. *AIDS Res. Hum. Retroviruses* 11, 501–508.

Mori, K., Ringler, D. J., Kodama, T., and Desrosiers, R. C. (1992). Complex determinants of macrophage tropism in env of simian immunodeficiency virus. *J. Virol.* 66, 2067–2075.

Platt, E. J., Wehrly, K., Kuhmann, S. E., Chesebro, B., and Kabat, D. (1998). Effects of CCR5 and CD4 cell surface concentrations on infections by macrophagetropic isolates of human immunodeficiency virus type 1. *J. Virol.* 72, 2855–2864.

Postler, T. S., and Desrosiers, R. C. (2013). The tale of the long tail: the cytoplasmic domain of HIV-1 gp41. *J. Virol.* 87, 2–15.

Reed, L. J., and Muench, H. (1938). A simple method of estimating fifty per cent endpoints. *Am. J. Epidemiol.* 27, 493–497.

Rerks-Ngarm, S., Pitisuttithum, P., Nitayaphan, S., Kaewkungwal, J., Chiu, J., Paris, R., et al. (2009). Vaccination with ALVAC and AIDSVAX to prevent HIV-1 infection in Thailand. *N. Engl. J. Med.* 361, 2209–2220.

Takeuchi, Y., Mcclure, M. O., and Pizzato, M. (2008). Identification of gammaretroviruses constitutively released from cell lines used for human immunodeficiency virus research. *J. Virol.* 82, 12585–12588.

Tamura, K., Peterson, D., Peterson, N., Stecher, G., Nei, M., and Kumar, S. (2011). MEGA5: molecular evolutionary genetics analysis using maximum likelihood, evolutionary distance, and maximum parsimony methods. *Mol. Biol. Evol.* 28, 2731–2739.

Vzorov, A. N., Gernert, K. M., and Compans, R. W. (2005). Multiple domains of the SIV Env protein determine virus replication efficiency and neutralization sensitivity. *Virology* 332, 89–101.

Vzorov, A. N., Weidmann, A., Kozyr, N. L., Khaoustov, V., Yoffe, B., and Compans, R. W. (2007). Role of the long cytoplasmic domain of the SIV Env glycoprotein in early and late stages of infection. *Retrovirology* 4, 94.

Wei, X., Decker, J. M., Liu, H., Zhang, Z., Arani, R. B., Kilby, J. M., et al. (2002). Emergence of resistant human immunodeficiency virus type 1 in patients receiving fusion inhibitor (T-20) monotherapy. *Antimicrob. Agents Chemother.* 46, 1896–1905.

Yoshimura, K., Shibata, J., Kimura, T., Honda, A., Maeda, Y., Koito, A., et al. (2006). Resistance profile of a neutralizing anti-HIV monoclonal antibody, KD-247, that shows favourable synergism with anti-CCR5 inhibitors. *AIDS* 20, 2065–2073.

Yusa, K., Maeda, Y., Fujioka, A., Monde, K., and Harada, S. (2005). Isolation of TAK-779-resistant HIV-1 from an R5 HIV-1 GP120 V3 loop library. *J. Biol. Chem.* 280, 30083–30090.

Yuste, E., Johnson, W., Pavlakis, G. N., and Desrosiers, R. C. (2005). Virion envelope content, infectivity, and neutralization sensitivity of simian immunodeficiency virus. *J. Virol.* 79, 12455–12463.

Yuste, E., Reeves, J. D., Doms, R. W., and Desrosiers, R. C. (2004). Modulation of Env content in virions of simian immunodeficiency virus: correlation with cell surface expression and virion infectivity. *J. Virol.* 78, 6775–6785.

Zhu, P., Chertova, E., Bess, J., Lifson, J. D., Arthur, L. O., Liu, J., et al. (2003). Electron tomography analysis of envelope glycoprotein trimers on HIV and simian immunodeficiency virus virions. *Proc. Natl. Acad. Sci. U.S.A.* 100, 15812–15817.

Zhu, P., Liu, J., Bess, J., Chertova, E., Lifson, J. D., Grisé, H., et al. (2006). Distribution and three-dimensional structure of AIDS virus envelope spikes. *Nature* 441, 847–852.

Conflict of Interest Statement: The authors declare that the research was conducted in the absence of any commercial or financial relationships that could be construed as a potential conflict of interest.

Received: 22 March 2013; accepted: 25 April 2013; published online: 14 May 2013.

Citation: Kuwata T, Takaki K, Enomoto I, Yoshimura K and Matsushita S (2013) Increased infectivity in human cells and resistance to antibody-mediated neutralization by truncation of the SIV gp41 cytoplasmic tail. Front. Microbiol. 4:117. doi: 10.3389/fmicb.2013.00117

This article was submitted to Frontiers in Virology, a specialty of Frontiers in Microbiology.

BIOCHEMISTRY
including biophysical chemistry & molecular biology

Article

pubs.acs.org/biochemistry

Effects of DNA Binding of the Zinc Finger and Linkers for Domain Fusion on the Catalytic Activity of Sequence-Specific Chimeric Recombinases Determined by a Facile Fluorescent System

Wataru Nomura,*[,†] Akemi Masuda,[†,‡] Kenji Ohba,[§] Arisa Urabe,[†] Nobutoshi Ito,[‡] Akihide Ryo,[∥] Naoki Yamamoto,[§] and Hirokazu Tamamura*[,†,‡]

[†]Institute of Biomaterials and Bioengineering, Tokyo Medical and Dental University, 2-3-10 Kandasurugadai, Chiyoda-ku, Tokyo 101-0062, Japan

[‡]Graduate School of Biomedical Science, Tokyo Medical and Dental University, 1-45 Yushima, Bunkyo-ku, Tokyo 113-8510, Japan

[§]Department of Microbiology, Yong Loo Lin School of Medicine, National University of Singapore, Singapore 117597, Singapore

[∥]Department of Microbiology and Molecular Biodefense Research, School of Medicine, Yokohama City University, 3-9 Fukuura, Kanazawa-ku, Yokohama 236-0004, Japan

Supporting Information

ABSTRACT: Artificial zinc finger proteins (ZFPs) consist of Cys_2-His_2-type modules composed of ~30 amino acids with a $\beta\beta\alpha$ structure that coordinates a zinc ion. ZFPs that recognize specific DNA target sequences can substitute for the binding domains of enzymes that act on DNA to create designer enzymes with programmable sequence specificity. The most studied of these engineered enzymes are zinc finger nucleases (ZFNs). ZFNs have been widely used to model organisms and are currently in human clinical trials with an aim of therapeutic gene editing. Difficulties with ZFNs arise from unpredictable mutations caused by nonhomologous end joining and off-target DNA cleavage and mutagenesis. A more recent strategy that aims to address the shortcomings of ZFNs involves zinc finger recombinases (ZFRs). A thorough understanding of ZFRs and methods for their modification promises powerful new tools for gene manipulation in model organisms as well as in gene therapy. In an effort to design efficient and specific ZFRs, the effects of the DNA binding affinity of the zinc finger domains and the linker sequence between ZFPs and recombinase catalytic domains have been assessed. A plasmid system containing ZFR target sites was constructed for evaluation of catalytic activities of ZFRs with variable linker lengths and numbers of zinc finger modules. Recombination efficiencies were evaluated by restriction enzyme analysis of isolated plasmids after reaction in *Escherichia coli* and changes in EGFP fluorescence in mammalian cells. The results provide information relevant to the design of ZFRs that will be useful for sequence-specific genome modification.

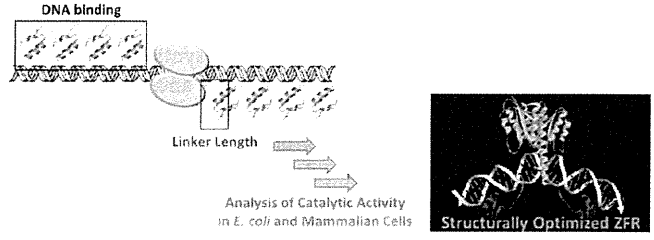

Artificial zinc finger proteins (ZFPs) can be used to engineer DNA binding domains with high specificity for desired target sequences, and ZFPs are a promising technology for gene therapy.[1−6] Modular assembly of ZFPs can create a DNA binding domain that targets virtually any sequence in the human genome.[3−5] By linking ZFPs to the catalytic domains of DNA-modifying enzymes, novel enzymes, including nucleases,[6] recombinases,[7−12] and methylases,[13−20] have been fabricated. These enzymes are endowed with programmable DNA binding specificity provided by the zinc finger protein fusion. Relevant to our development of ZFRs, recombinase enzymes from the serine recombinase family have been well studied.[21] In comparison with members of the tyrosine recombinase family such as Cre and Flp recombinases, the serine recombinases, including Tn3 and $\gamma\delta$ resolvases, Hin invertase, and Gin invertase, have DNA binding domains that are structurally independent of the catalytic domain. The structures of the catalytic domains and the sequences required for catalytic activity are highly conserved in these recombinases.[22] Tn3 and $\gamma\delta$ are among the best-characterized site-specific recombinase enzymes in the serine recombinase family. Only 35 amino acid residues differ between the $\gamma\delta$ and Tn3 resolvases, and their structures and functions are similar.[23] Negatively supercoiled DNA is a prerequisite for substrate recombination with native serine recombinase enzymes.[21] Although it is known that native serine recombinases require accessory proteins binding to sites I−III, activating mutants that require only the 28 bp of site I for successful recombination have been isolated.[7] In these hyperactivated enzymes, a DNA substrate in the form of negatively supercoiled DNA is not required for activity, and this allows application of activated catalytic domains with ZFPs to create zinc finger recombinases (ZFR). It has been suggested that reactions with serine recombinases proceed in three

Received: December 19, 2011
Revised: January 21, 2012
Published: January 23, 2012

steps: (i) formation of a dimer binding to the two forms of site I on the DNA, (ii) formation of a tetramer between the forms of site I, and (iii) strand exchange.[24,25] After the strand exchange reaction, the sequences between target sites are excised and the strands ligated (Figure 1).

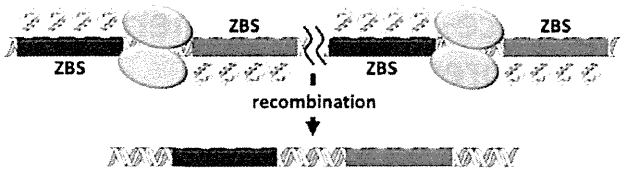

Figure 1. Schematic illustration of the ZFR reaction at a target site. The green and red boxes represent zinc finger binding sites (ZBSs). The yellow spheres represent catalytic domains of Tn3 resolvase.

ZFRs based on catalytic domain variants of Tn3, Gin, and Hin fused to artificial ZFPs have been shown to catalyze site-specific recombination in *Escherichia coli*[7−11] and mammalian cells.[8,9,11,12] ZFRs have also been shown to catalyze high-fidelity site-specific integration in mammalian cells.[9,11,12] While directed evolution of recombinase catalytic domains has proven to be essential for developing ZFR enzymes that function in mammalian cells, other aspects of ZFR design have not been thoroughly studied. In this report, we have synthesized ZFR mutants with variable numbers of zinc fingers and studied the role of peptide linkers that connect the Tn3 resolvase catalytic domain with the ZFP DNA binding domain. These effects are not readily addressed using molecular evolution strategies. For facile evaluation of recombination reactions in mammalian cells, a system that allows evaluation within 48 h was developed utilizing DsRed expression as a marker of transfection efficiency and EGFP expression as a marker of recombination efficiency. The results obtained revealed the optimal structures of the ZFRs, and the recombination efficiency results for linker mutants were verified by modeling studies.

■ EXPERIMENTAL PROCEDURES

Construction of ZFP Genes. ZFP genes were constructed as described previously.[26,27] Briefly, plasmid pc3XB encoding ZFPs purchased from Addgene (http://www.addgene.org) was repeatedly ligated. The zinc finger gene that was obtained was inserted into pMAL-p4x as an *Xba*I−*Bam*HI fragment for protein expression. A minor change was made to the multiple cloning site of pMAL-p4x (Figure S1 of the Supporting Information).

Target Enzyme-Linked Immunosorbent Assays (ELISAs). ELISA wells of 96-well plates were coated by incubation with 25 μL of 8 ng/mL streptavidin in PBS for 1 h at 37 °C. The plates were washed twice with dH_2O, and 25 μL of 5′-biotinylated hairpin oligonucleotide target in zinc buffer A (ZBA) [10 mM Tris-HCl (pH 7.5), 90 mM KCl, 1 mM $MgCl_2$, and 90 μM $ZnCl_2$] was added. After incubation for 1 h at 37 °C, plates were washed twice with dH_2O. Blocking solution (ZBA with 3% BSA, 175 μL) was added, and incubation continued for 1 h at 37 °C. The blocking solution was then removed; 25 μL of purified protein in ZBA was added, and 2-fold serial dilutions were performed into 1% BSA, 5 mM DTT, and 10 ng/μL salmon sperm DNA in ZBA. After incubation for 1 h at room temperature, the plates were washed 10 times with dH_2O and the monoclonal anti-MBP antibody (Sigma-Aldrich, 1:1000 dilution by ZBA with 1% BSA, 25 μL) was added. After incubation for 30 min at room temperature, the plates were washed 10 times with dH_2O and a diluted secondary anti-mouse IgG AP conjugate (Sigma-Aldrich, 1:1000 dilution by ZBA with 1% BSA, 25 μL) was added. After incubation for 30 min at room temperature, plates were washed 10 times with dH_2O. The alkaline phosphatase reaction was performed with *p*-nitrophenylphosphate for 30 min, and the absorbance at 405 nm was read with a microplate reader. The data were collected and plotted. The data were fit to the equation $y = 1/(1 + K_d/x)$, where y is the proportion of bound MBP−ZFP fusion protein to maximal binding derived from the absorbance at 405 nm and x is the concentration of the MBP−ZFP fusion protein. The K_d values are averages of three or more independent experiments, and standard errors of the mean (SEM) are shown.

Construction of ZFR Substrates. Each substrate plasmid contained a recombination cassette composed of two ZFR recombination sites flanking an EGFP gene as a stuffer sequence. Cassettes were assembled by amplifying the EGFP gene with primers encoding the ZFR site. The polymerase chain reaction (PCR) product was cloned into pAra-OP.[20] ZFP genes were amplified by PCR from plasmid pc3XB and inserted into the plasmid as *Eco*RI−*Sac*I fragments. Plasmids that contained ZFR with Gly-Ser linkers were mutated at the *Bst*BI site before insertion of the catalytic domain.

Construction of ZFR Genes. The DNA fragment of the Tn3 resolvase catalytic domain was amplified from pWL625 (ATCC accession number 31787) utilizing 5′-GAGGAG-GAATTCATGCGACTTTTTGGTTACGCT-3′ and 5′-GAG-GAGAAGCTTTCACGAGGCCCTTTCGTCTT-3′ as primers. The fragment was inserted into pBluescriptSK(−) as an *Eco*RI−*Hin*dIII fragment. Tn3-activating mutations (R2A, E56K, G101S, D102Y, M103I, and Q105L) were introduced into the Tn3 encoding gene. Linker sequences were amplified via PCR with the Tn3 fragment by primers that included the linker sequence. Tn3 fragments with different linkers were digested with *Eco*RI and *Bgl*II and ligated into similarly digested pAra-OP with the EGFP and ZFR sites. Tn3 fragments with various Gly-Ser linkers were also digested with *Eco*RI and *Bst*BI and then ligated. The plasmids were maintained with chloramphenicol.

Assay of Recombination of Plasmids in *E. coli*. The plasmid with a ZFR gene downstream from the arabinose promoter and the substrate sequences were introduced into *E. coli* by electroporation. After incubation for 14 h at 37 °C on an LB-agar plate, colonies were picked up and grown for 14 h at 37 °C in LB medium. Purified plasmids were digested with *Eco*RI for 1 h at 37 °C. After electrophoresis on a 0.8% agarose gel, the fragment intensity was estimated with ImageJ (Figure S2 of the Supporting Information).

Recombination Reaction of ZFR in Mammalian Cells. The EGFP gene, flanked by recombination sites, was inserted between *Nhe*I and *Kpn*I in pcDNA5/FRT (Life Technologies). A double-stranded oligonucleotide encoding the upstream target site was inserted into the *Mlu*I site, and the other oligonucleotide for the downstream target site was inserted into *Kpn*I and *Bam*HI sites. Cotransfection of the substrate plasmid and Flp expression plasmid (pOG44, Life Technologies) allowed site-specific integration into the single FLP recombinase target (FRT) site present in the Flp-In-CHO cell line (Life Technologies). Colony-acquired hygromycin resistance was characterized by fluorescently activated cell sorting (FACS) and genomic PCR. The sequence of the target site was confirmed. Cells were maintained in Ham's F-12 containing 10% (v/v)

dx.doi.org/10.1021/bi201878x | *Biochemistry* 2012, 51, 1510−1517

Table 1. DNA Binding Affinities of ZFPs

	two fingers	three fingers	four fingers	five fingers	six fingers
K_d (nM)[a]	160±20	23.6±3.6	12.8±1.1	15.4±1.4	12.9±1.4
R^2	0.90	0.87	0.94	0.94	0.94

[a]The values are averages of three or more independent experiments.

FBS and antibiotics (Wako Chemicals). The DsRed expression vector was constructed as follows; a DsRed-monomer sequence was ligated into pIRES2-EGFP (Clontech) to substitute for EGFP, and a Tn3-ZFP-NLS fragment was inserted between *Nhe*I and *Eco*RI in pIRES2-DsRed. On the following day, after 2×10^5 cells had been seeded, the ZFR expression vector was transfected into cells using Lipofectamine LTX Reagent and PLUS Reagent (Life Technologies). After being transfected for 48 h, cells were collected and analyzed by flow cytometry.

Molecular Modeling of the Linker Variants of ZFR. Computer models were generated using Discovery Studio (Accelrys Inc.). The crystal structure of the $\gamma\delta$ resolvase–DNA complex [Protein Data Bank (PDB) entry 1GDT][22] was manually mutated in the protein and DNA to match the molecules used in this study. The first zinc finger module, obtained from a zinc finger–DNA complex (PDB entry 1MEY),[28] was placed on the resolvase–DNA complex by superimposing the phosphate backbone atoms of corresponding DNA residues. Appropriate linker atoms were then added and optimized by simulated annealing and energy minimization. During this optimization, the atoms in the resolvase, zinc fingers, and DNA were fixed, allowing only linker atoms to move.

■ RESULTS

Construction of Zinc Fingers and DNA Binding Analyses. The 18 bp target sequence of the zinc finger protein utilized in this study was 5′-CTGCATGCACTGGATGCA-3′.

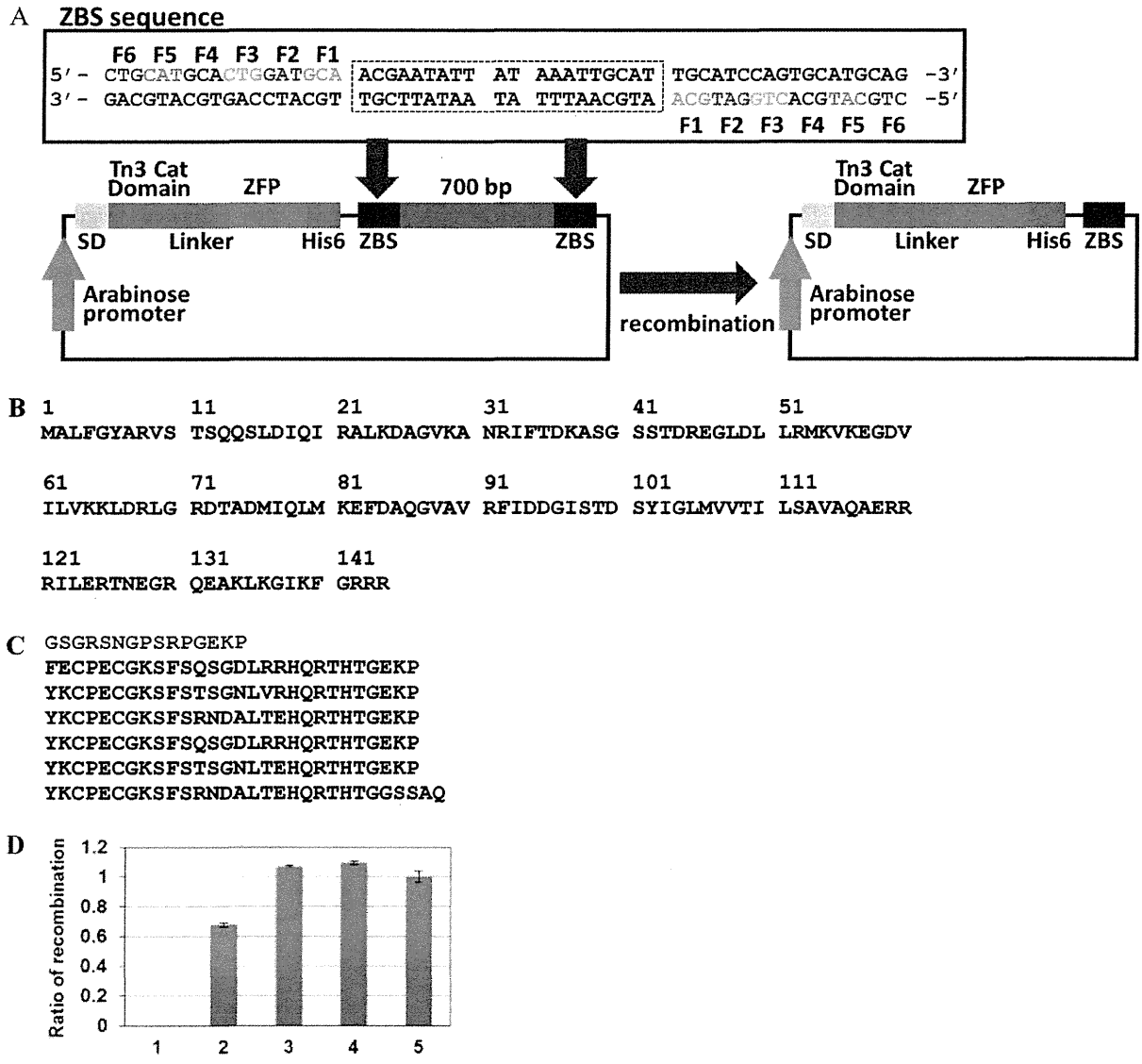

Figure 2. (A) Schematic of recombination at zinc finger binding sites (ZBSs). Recombination results in smaller plasmids. ZBS sequences are shown in the box. SD represents the Shine-Dalgarno sequence. (B) Amino acid sequences of the hyperactivated Tn3 catalytic domain. (C) Amino acid sequences of the linker (red) and six-zinc finger domain utilized for the analysis in *E. coli*. (D) Recombination efficiency depends on the number of fingers in ZFR. Columns 1–5 show the recombination efficiencies of two- through six-finger modules. The ratios are relative to the efficiency of the six-finger module. The error bars show the SEM of three or more independent experimental results.

A

```
Clone 1.          R RSNGPSRPGEKP
Clone 2. IKF      R RSNGPSRPGEKP
Clone 3. IKF GRRR
Clone 4. IKF GRRR EKP
Clone 5. IKF GRRR RPGEKP
Clone 6. IKF GRRR GPSRPGEKP
Clone 7. IKF GRRR RSNGPSRPGEKP
Clone 8. IKF GRRR GSGRSNGPSRPGEKP
Clone 9. IKF GRRR GSGGGSRSNGPSRPGEKP
Clone 10.IKF GRRR GSGGGSGGSRSNGPSRPGEKP
Clone 11.IKF GRRR GSGGGSGGSGGSRSNGPSRPGEKP
Clone 12.IKF GRRR GSGGGSGGSGGSGGSRSNGPSRPGEKP
Clone 13.IKF GRRR GSGGGSGGSGGSGGSGGSRSNGPSRPGEKP
Clone 14.IKF GRRR GSG
Clone 15.IKF GRRR GSGGGS
Clone 16.IKF GRRR GSGGGSGGS
Clone 17.IKF GRRR GSGGGSGGSGGS
Clone 18.IKF GRRR GSGGGSGGSGGSGGS
Clone 19.IKF GRRR GSGGGSGGSGGSGGSGGS
```

B

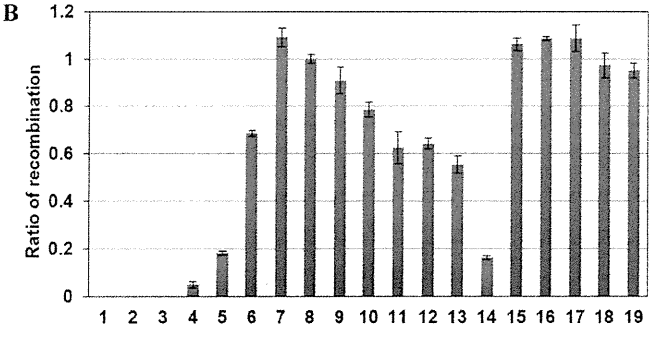

Figure 3. (A) Amino acid sequences of linkers of clones. All linkers were tested in the context of six-finger binding domains. (B) Results of recombination efficiency of clones with different linker sequences. The numbers of columns correspond to the clone numbers as described in panel A. The ratios are relative to the efficiency of clone 8. The error bars show the SEM of three or more independent experimental results.

Zinc fingers were constructed on the basis of a modular assembly strategy described by Barbas and co-workers.[27,29–32] Two- to six-finger proteins were constructed to obtain DNA binding domains with different affinities. Proteins were expressed as maltose binding protein fusions and purified with an MBPTrap column (GE Healthcare). The purity of the proteins was determined to be >90%. The DNA binding affinities were evaluated by an ELISA with the biotinylated hairpin oligonucleotide as a target.[10] The binding constants (K_d) of the two-, three-, four-, five-, and six-finger modules, listed in Table 1, were found to be 160, 23.6, 12.8, 15.4, and 12.9 nM, respectively. These results indicate that in the two-, three-, and four-finger modules, the DNA binding affinity increased with finger number but the binding affinities of ZFPs with four, five, and six fingers were similar.

Construction of ZFR Chimeric Proteins and Recombination Analysis in *E. coli*. The target DNA sequence of ZFR is shown in Figure 2A. The target site consists of a 20 bp spacer sequence flanked by 18 bp zinc finger binding sites. The spacer region was previously shown to be a Z+4 site in the target spacer of Z-resolvase.[7] For the evaluation of recombination in *E. coli*, a plasmid-based recombination system was constructed. The coding sequence of ZFRs was inserted into the plasmid containing a 700 bp stuffer sequence flanked with target sequences. In the recombination mediated by the expressed ZFRs, the stuffer sequence is excised to produce a smaller plasmid (Figure 2A). The amino acid sequences of the hyperactivated Tn3 catalytic domain, the linker between the domains, and the zinc finger domain are shown in panels B and C of Figure 2. The recombination efficiency was evaluated by a restriction enzyme assay. Plasmid purified from *E. coli* was digested by *Eco*RI, which is a single cutter of the plasmid. The linear plasmid was analyzed on an 0.8% agarose gel, and the fractions of the longer (nonrecombinant) and shorter (recombinant) plasmids were evaluated (Figure S2 of the Supporting Information). ZFR variants with different numbers of fingers were evaluated in this recombination system, and recombination ratios increased with increasing numbers of fingers from two to four fingers. The values of recombination efficiencies for ZFRs with four to six fingers were similar, reflecting the DNA binding affinities (Figure 2D). The production of recombinant sequence was confirmed by DNA sequencing analysis (Figure S3 of the Supporting Information).

In the next study, the reactions of ZFR variants with different linker lengths in the context of the six-finger module were tested (Figure 3B). In this experiment, 19 constructs were prepared. The variants were categorized into three groups depending on lengths and the compositions of linker sequences. The first group variants have short linkers with deletions within the catalytic

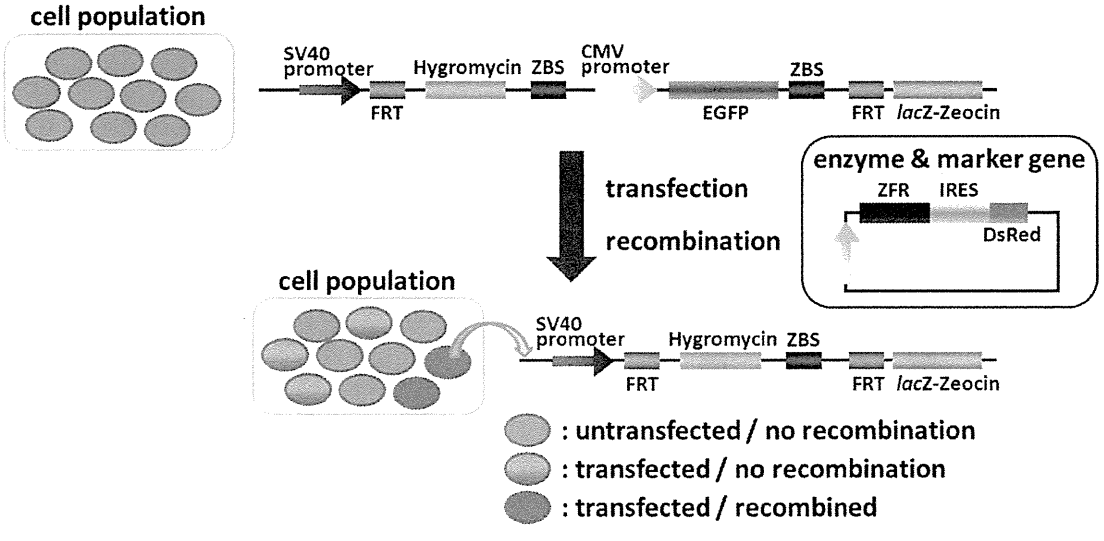

Figure 4. Recombination system constructed utilizing Flp-In-CHO-K1 cells.